Summer 2010

Investigation of the roles of Kinesin-5 motor protein family members in *Arabidopsis thaliana*

Bareza Abbas Rasoul
James Madison University

Investigation of the Roles of Kinesin-5 Motor Protein Family Members in *Arabidopsis thaliana*

Bareza Abbas Rasoul

A thesis submitted to the Graduate Faculty of

JAMES MADISON UNIVERSITY

In

Partial Fulfillment of the Requirements

for the degree of

Master of Science

Biology

August 2010

Dedication

Dedicated to my parents, Abbas and Glizar Rasoul who hope and dream too much for their children and not enough for themselves.

Acknowledgements

This work would have not been completed without help from supernatural and natural forces for which I am thankful. I really appreciate my advisor, Dr. Bannigan, who reared me to graduation while rearing her baby daughter Imogen, to toddlerhood. I am at awe at all she knows and all she does but still manage to have time for students.

I also thank my committee members Dr. Daniel, Dr. Halsell and Dr. Monroe for just agreeing to guide and critique this project. The answers to their inquisitive questions make up a good part of this thesis. I would like especially to thank Dr. Monroe who helped greatly by offering ideas, expertise and, unintentionally, material and lab space. Thanks also to all my teachers who had more influence on me than I or they might realize.

The work on this thesis would have taken quite a while longer had it not been for the needed, meticulous hands of Sarah Fargis. I thank her for giving hope when the end was so hopelessly afar.

My thanks goes out to the donor, Dr. Bannigan, and baker, Java city, of the banana bread which nourished me through the long hours when I was ‘going bananas’ trying to type words that sounded like monkey language.

Lastly, I would like to thank all those who cared about this project and contributed, even with as little as a show of interest in the form of a question.

Table of Contents

List of tables

List of figures

Abstract

Eukaryotic cells contain a cytoskeleton that performs a range of essential functions, including intracellular transport, nuclear division and shaping the cell. There are various kinesin motor proteins involved in organizing the microtubule cytoskeleton during interphase and mitosis. The plant *Arabidopsis thaliana* has the largest number of kinesins amongst all sequenced organisms. Many of those kinesins have not been studied. Members of the Kinesin-5 family cross link microtubules and are crucial for separation of mitotic spindle poles. There are 4 members of this family in Arabidopsis: Kinesin-5 A, B, C and D, but only Kinesin-5 C has been studied previously. Each animal species only has either one or two of Kinesin-5 members, which have been well studied and can be used as a reference for other Kinesin-5 proteins. There is evidence that some functions are conserved between Kingdoms; however the multiple family members in Arabidopsis suggests that Kinesin-5 motors play some roles unique to plants. We have characterized T-DNA insertion lines of Arabidopsis Kinesin-5 A, B and D genes, two of which (A and B) are knockout mutants. Our analysis of growth rates, cortical microtubules, mitotic indexes, mitotic arrays, trichome morphology and pavement cell morphology indicates that Kinesin-5 A and Kinesin-5 B perform some different, and relatively minor functions in Arabidopsis growth and development. Kinesin-5 A appears to stabilize microtubule bundles in leaf epidermal pavement cells. Kinesin-5 B affects root growth rate, possibly through the organization of cortical microtubules in the root. Kinesin-5 A and B also play roles in mitosis. We propose that the third Kinesin-5 member, Kinesin-5 D, is an essential protein and for that reason we were unable to recover any homozygous mutants.

I. Introduction

The Cytoskeleton

All eukaryotic cells contain cytoskeleton proteins that perform a variety of functions in many cellular processes including cell structure, intracellular transport, motility and cell division. The cytoskeleton is primarily composed of three filamentous proteins: microtubules, intermediate filaments and actin filaments, which differ in structure, size and function. The most conserved cytoskeleton proteins amongst all eukaryotes are the actin filaments and the microtubules (Reddy and Day, 2001). Actin is important for maintaining cell shape, vesicular transport, cell division, cell motility and phagocytosis (Wasteneys and Yang, 2004). Microtubules also perform some of the same tasks, in addition to positioning organelles, forming the mitotic and meiotic spindles, and constructing motile structures such as flagella and cilia (Gelfand and Bershadsky, 1991). During mitosis and meiosis, cells utilize the cytoskeleton to perform cell shape changes, organelle distribution, chromosome separation and cytokinesis.

Microtubules

Microtubules are polymers of alpha and beta tubulin subunits, which polymerize to form a long, hollow, tubular structure that is resistant to bending (Gelfand and Bershadsky, 1991). The tubulin subunits polymerize in an alternating pattern. One end of the microtubule begins with alpha-tubulin while the other end of the tube ends with beta-tubulin. This structural make-up gives the microtubule an intrinsic polarity. The beta-tubulin end of the microtubule protein is designated as the “plus end” while the alpha-tubulin end is called the “minus end.” At the plus end, tubulin polymerization and depolymerization occurs at a fast pace while at the minus end, polymerization and depolymerization happens at a slower rate or not at all. If the minus end of the

microtubule is not anchored to a microtubule-organizing center, the addition and removal of tubulin can happen constantly at both ends and so the microtubule is a highly dynamic structure (Desai and Mitchison, 1997; Vassileva *et al*., 2005; Guo *et al*., 2009).

The nucleation of microtubule polymerization differs depending on the type of cell. In animal cells, microtubule elongation originates from an organelle known as the centrosome, which acts as a microtubule-organizing center (Kellogg *et al.,* 1994). The minus ends of the microtubules are anchored to the microtubule-organizing center and the dynamic plus ends radiate to the periphery of the animal cell. Plants do not possess distinct microtubule-organizing centers. Microtubules originate from the nuclear surface, from dispersed points in the cytoplasm and from the cell plasma membrane (Schmit, 2002). The nucleated microtubules are arranged to form different structures during interphase, mitosis, and the formation of specialized cell shapes.

Interphase

During interphase in plants and animals, microtubules spread throughout the cell, acting as tracks for the transport of organelles and for cytoskeleton rearrangements using motor proteins (Hashimoto, 2003). In plants, the interphase microtubules lie close to the cell membrane in the cell cortex. In elongating plant cells, microtubules are organized parallel to each other (Ehrhardt and Shaw, 2006). They guide the deposition of cellulose microfibrils in the cell wall, thus influencing cell wall properties and cell expansion (Baskin, 2001; 2005). The close associations of the microtubules and the cell membrane allows for controlled relief of turgor pressure, which is the main osmotically regulated force that expands plant cells, by facilitating cell wall reshaping (Wasteneys and Ambrose, 2009). Cortical microtubules are rearranged for many purposes and through

these modifications they aid in various cell processes such as cell shape determination and expansion (Wasteneys and Ambrose, 2009). The dynamics of these cortical microtubules affects cell growth (Mathur and Chua, 2000). Stable microtubules in trichomes reorient with respect to the longitudinal growth axis and initiate branch formation (Mathur and Chua, 2000). Similarly, in root hairs, when microtubules are either stabilized or destabilized using taxol or oryzalin respectively, the root hairs become wavy, grow in different directions or form multiple tips (Bibikova *et al*., 1999).

Organization of the cortical array has important implications for the morphology of the plant. This has been studied most extensively in roots and specialized cells like pavement cells and trichomes. Microtubules self-organize passively into parallel arrays; however, maintaining an orientation transverse to the direction of elongation is an active process (Lagomarsino *et al*., 2007). This could be achieved by microtubule associated proteins and/or motor proteins. In elongating root cells microtubules are parallel to each other and transverse to the direction of elongation (Baskin *et al*., 1999). In roots, disorganization or fragmentation of the cortical microtubule array often results in swelling and reduced elongation of the root. A temperature sensitive mutant of a microtubule associated protein, MOR1, a protein that controls microtubule dynamics, shows swollen root cells and disorganized cortical microtubules (Whittington *et al*., 2001). Microtubule severing protein mutant *Fra2/Bot1* (Burk *et al*., 2001; Bichet *et al*., 2001) has swollen root cells and disordered cortical microtubules as well. Many other mutations of microtubule associated proteins and the alpha and beta tubulin proteins affect microtubule organization and so the overall structure of the cells and plant (Buschmann and Lloyd, 2008).

Specialized cell shapes

In the past decade, morphogenesis of leaf epidermal cells, trichomes, root hairs and stomata has been studied to better understand cell shape determination (Qian *et al.*, 2009). Cells differentiate into distinct shapes to perform their specific functions. Arabidopsis leaf trichomes (leaf hairs) which are single cells with multiple extensions (branches) protect the leaf from some herbivorous attacks (Loughner *et al*., 2010). They are the first cells to differentiate on the developing leaf primordia (Larkin *et al*., 1996), after which they go through endoreduplication (multiple S-phase cycles without mitosis) approximately four times (Hülskamp *et al*., 1994) and form two branches. These two branches are parallel to the long axis of the leaf. A third trichome branch is formed on the branch that points to the tip of the leaf (Folkers *et al*., 1997). The trichome later enlarges by vacuolization (Schwab *et al*., 2000). These shape changes and enlargements require the reorganization of the cytoskeleton. The reorganization guides the layout of cellulose microfibrils in the wall which influences cell expansion patterns (Smith and Oppenheimer, 2005). The trichomes of cytoskeleton mutants can be short, swollen, or have fewer branches compared to the wild type (Mathur, 2004). Microtubule mutants tend to have reduced trichome branching while actin mutants have short, swollen trichomes (Mathur, 2004).

The leaf epidermal cells, called pavement cells, are shaped like puzzle pieces that interlock to contain the mass of the leaf, prevent loss of moisture, and resist pathogen invasion (Qian *et al.*, 2009). They differentiate in three stages (Fu *et al*., 2002) (Figure 1). A small cell expands along the leaf axis and begins to form indentations and outgrowths laterally into adjacent cells. These outgrowths take the form of shallow lobes. The lobes

later become well defined with a clear neck region and the lobes on neighboring cells form in the troughs between them. This results in neighboring cells that have interlocking cell extensions (Fu *et al*., 2002).

The cytoskeleton plays an important role in forming the shape of pavement cells (Smith and Oppenheimer, 2005). Microtubule bundles are aligned transversely in the neck region of the lobe and the initiating and expanding lobes are rich in fine actin microfilaments (Wasteneys *et al*., 1997) (Figure 1). Pavement cells with disorganized microtubules have wide neck areas and less interdigitation between cells (Fu *et al*., 2002), which leads to a low perimeter to area ratio. Co-ordination of the placement of the lobes and troughs of each cell, and the cytoskeleton that guides them, is controlled by a Rho GTPase signaling pathway known to be involved in cell expansion in animals, and recently found in plants (Fu *et al*., 2005).

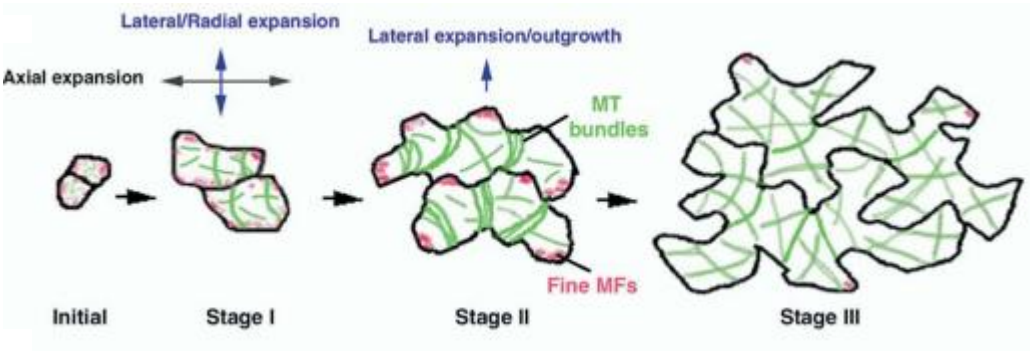

Figure 1. A schematic illustration of Arabidopsis leaf pavement cell development and associated fine actin microfilaments (red patches) and microtubules (green lines) in the cortex based on a previous description (Fu *et al*., 2002). Arrows indicate directions of expansion (Fu *et al*., 2005).

Through a mutation, it was found that a plant Rho GTPase (ROP) (Jaffe and Hall, 2005) is part of the pathway that initiates lobing in developing pavement cells (Fu *et al*., 2002) by promoting microtubule bundling in some areas, which restricts lobe formation, while in other areas disorganization of microtubules allows lobe formation (Fu et *al*., 2005). For example, the MOR1 mutant, which has disorganized microtubules, has pavement cells with reduced lobing and reduced microtubule bundling (Kotzer and Wasteneys, 2006).

Mitosis

The plant cell cycle is largely similar to the animal cell cycle: the chromosomes condense (prophase) and are aligned at the cell midplate (metaphase) before the sister chromatids are separated (anaphase) to form into two daughter nuclei (telophase), and finally the cytoplasm is partitioned into two daughter cells (cytokinesis) (Lebedeva *et al*., 2004) (Figure 2). Microtubules are essential for nuclear division and daughter cell separation during mitosis and cytokinesis (Kost *et al*., 1999; Hepler and Hush, 1996). To accomplish the partitioning of genomic and cytosolic material during the different stages of the cell cycle, the microtubules have to be arranged into various arrays, some of which differ between plant and animal cells (Figure 2).

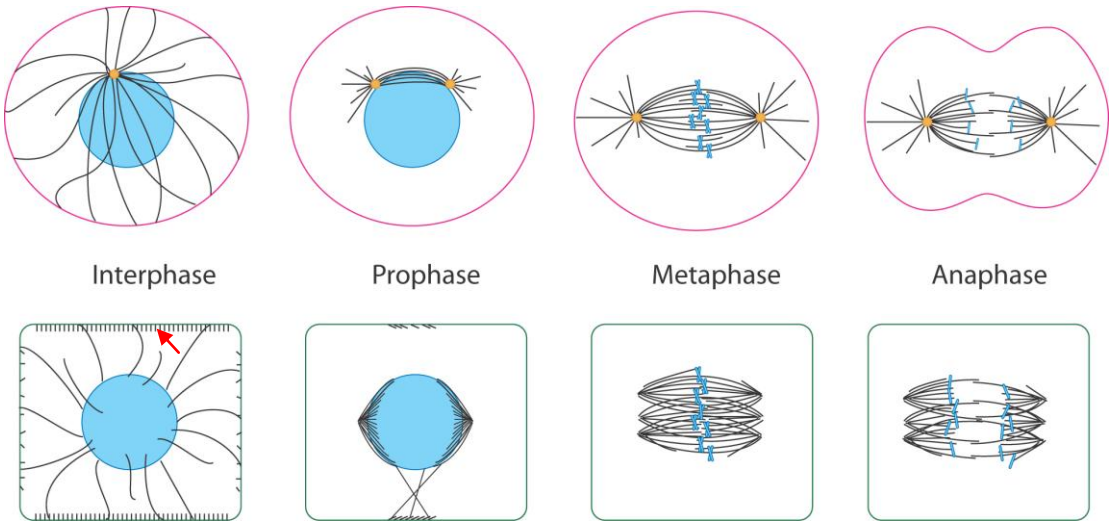

Figure 2. Illustration of mitotic stages of animal (top row) and plant (bottom row) cells. Microtubules are indicated in black, DNA is blue and centrosomes are yellow. Notable differences between the microtubule arrays in plant and animal mitosis are the lack of centrosomes and presence of a pre-prophase band (red arrow) in plants (Illustration from Bannigan *et al*., 2008).

Prophase

The microtubule array during prophase differs in animal and plant cells. In animal cells, the microtubules arrange into two astral poles on opposite sides of the nucleus (Lloyd and Chan, 2006). In plants, the start of mitosis is marked by the formation of a pre-prophase band, and as the cell enters prophase, astral poles form on the nuclear envelope. The pre-prophase band is a thick band of microtubules surrounding the middle of nucleus and lying close to the cell membrane. The placement of the pre-prophase band forecasts the future location of the new cell wall formed between daughter cells (Mineyuki, 1999). The pre-prophase band forms by stabilizing pre-existing interphase microtubules in the region of the band and/or by destabilizing the surrounding cortical microtubules (Müller *et al.,* 2009).

Metaphase and Anaphase

When the nuclear envelope breaks down, the microtubules are rearranged to form the mitotic spindle. The spindle array is similar in animal and plant cells, with microtubules emanating from the spindle poles towards the chromosomes, which they then capture and align in the middle of the cell in one plane, called the metaphase plate. In animals, there is a centrosome from which microtubule nucleate on either end of the spindle but in plants, which lack centrioles, the microtubule nucleating site is more diffuse (Seltzer *et al*., 2003; Schmit, 2002). As a result, plant spindles usually have broad ends while animal spindles have very focused ends. After the microtubules have attached to the chromosomes, the two sister chromatids come apart and are pulled towards the two ends of the mother cell. This mitotic stage is referred to as anaphase and is similar in plants and animals (Hayashi *et al*., 2007).

Telophase and Cytokinesis

When the sister chromosomes are separated to either end of the parent cell, nuclear envelopes re-form to create two daughter nuclei during telophase. This is followed by the division of the cytoplasm. This process of separation of the two daughter cells is called cytokinesis. Cytokinesis is different in animal and plant cells. In animal cells, an actin ring constricts to pinch the two daughter cells apart (Lloyd and Chan, 2006). In plant cells, the microtubules form a structure called the phragmoplast that starts in the middle of the plane of cell division and expands out to the edges of the cell in a ring (Zhang *et al*., 1990). The phragmoplast is made up of antiparallel microtubules that act as tracks to deliver building material to the cell plate for the new cell wall that will separate the daughter cells. As the phragmoplast expands out, the new cell wall is built from the center outward to the parental cell wall to join at the site where the pre-prophase band appeared at the beginning of mitosis (Müller *et al.*, 2009).

Motor Proteins

During mitosis the microtubules need to be rearranged to form the different mitotic arrays. The forces that move the microtubules are generated by molecular motor proteins. There are several types of molecular motors performing numerous functions to sustain the cell. The motors that move microtubules and transport cargo on microtubules include kinesins and dyneins.

Kinesins and dyneins have different motor properties. While dynein always moves towards the minus end of microtubules, different kinesins can move in either the positive or negative direction on microtubules (Reddy and Day, 2001). Plants do not have

dyneins (Lawrence *et al*., 2001), but they have many different kinesins that perform diverse functions in the cell.

Kinesins are a diverse group of motor proteins found in plants, animals and other eukaryotes (Richardson *et al.,* 2006). The functions of kinesins are various and include vesicle transport, cytoskeleton support, organization of the bipolar spindle and generation of mitotic spindle forces (Reddy and Day, 2001). Kinesins were first observed in squid axons in 1985 (Brady, 1985; Vale *et al.*, 1985). These motor proteins have been extensively studied in animals but much less so in plants. The first plant kinesins were found in the tobacco phragmoplast (Asada *et al.,* 1991) and the tobacco pollen tube (Cai *et al.,* 1993).

Kinesins in Sequenced Organisms

The genome of the plant *Arabidopsis thaliana* (L.) Heynh was sequenced between 1996 and 2000 by the Arabidopsis Genome Initiative (Kaul *et al*., 2000). Analysis of the genome revealed 61 kinesin motor protein-like sequences; more than in any other organism (Reddy and Day, 2001). Some have been categorized and are homologues of well-studied animal kinesins, but not all Arabidopsis kinesins have homologues in animals. Therefore, the unique plant kinesins could have specialized functions in the various microtubule arrays that are unique to plants (Dagenbach and Endow, 2004).

There are over 640 amino acid sequences of kinesins in GeneBank (Miki *et al.,* 2005) and 98 percent of these can be classified into one of the fourteen families generated using differences in the motor and neck regions (Lawrence *et al.,* 2004). The conventional kinesin protein is made of a globular motor domain, a coiled-coil stalk and a tail (Miki *et al.,* 2005).

Two kinesin families that are conserved amongst eukaryotes and which are crucial for spindle structure and function are the Kinesin-5 and Kinesin-14 class motors (Richardson *et al*., 2006). Kinesin-5 motors are homotetramers, consisting of two microtubule-binding motor domains at each end of a long, coiled stalk (Cole *et al.*, 1994) (Figure 3). The structure of the Kinesin-5 protein is such that it can bind to two parallel or anti-parallel microtubules and move toward the plus end of both of them simultaneously (Kapitein *et al.*, 2005). Motor proteins in the Kinesin-14 family, on the other hand, are dimers with two motor domains at one end and microtubule binding domains at the other end (Miki *et al*., 2005). Unlike Kinesin-5 motors, these motors move towards the minus ends of microtubules (Sharp *et al*., 2000) (Figure 3).

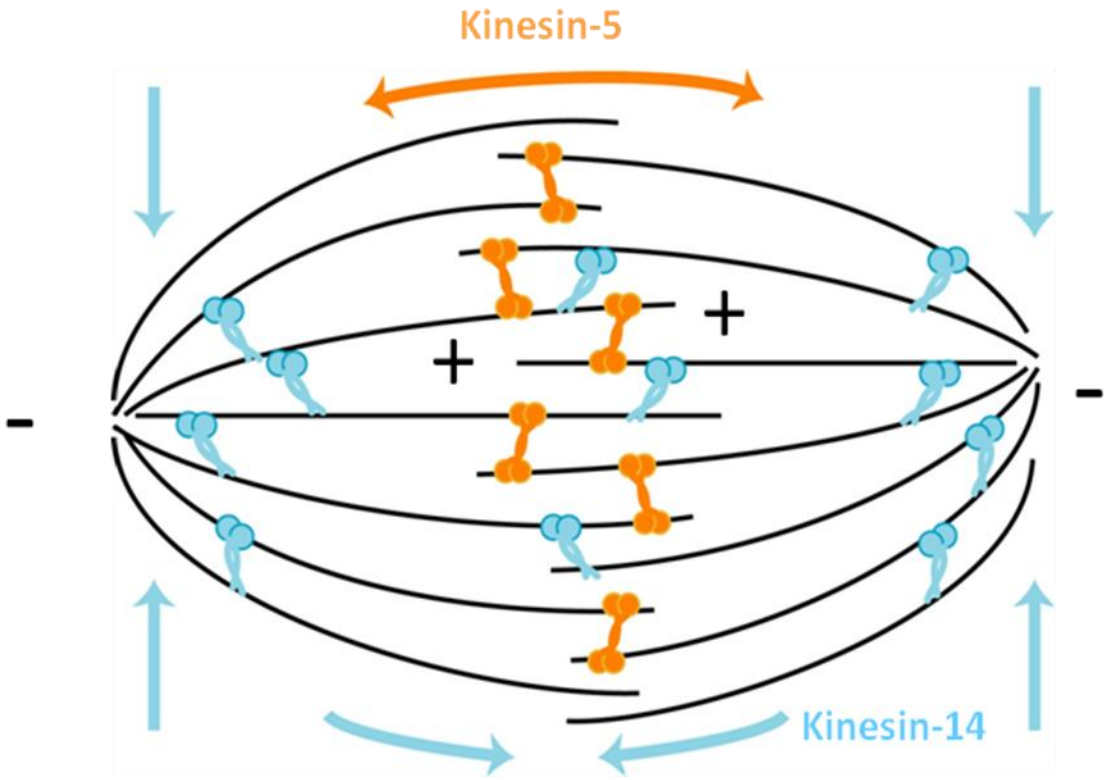

Figure 3. Illustration of mitotic spindle with Kinesin-5 and Kinesin-14 motor proteins, based on fungal and animal studies (Sharp *et al*., 2000; Ferenz *et al*., 2010; Gatlin and Bloom, 2010). Kinesin-14 proteins (blue) provide inward forces by walking towards the microtubule minus ends, while Kinesin-5 proteins (orange) generate outward forces by walking to the plus ends of two antiparallel microtubules simultaneously.

Function of Kinesins in Spindles

Kinesin motor proteins play important roles during mitosis, particularly in the formation and function of the spindle. The majority of the available information is from animal studies, and has been applied to homologous proteins in plants. The bipolar spindle is constructed and maintained by antagonistic forces generated primarily by Kinesin-14 family proteins and Kinesins-5 proteins (Sharp *et al*., 2000; Hentrich and Surrey, 2010)

Motors from the Kinesin-14 family focus the poles at the minus end of the microtubules in the spindle array and draw the two halves of the spindle towards each other (Hentrich and Surrey, 2010). When the sister chromatids are detached from each other, it is predominantly Kinesins-5 motors that push the spindle poles apart by cross linking antiparallel microtubules in the middle of the spindle and walking towards their positive ends (Kapitein *et al.*, 2005). In animals the function of Kinesin-5s is crucial for mitosis. When Kinesin-5 is inhibited the anaphase spindle collapses (Ferenz *et al*., 2010) leading to the session of mitosis.

In plants, Kinesin-5 protein is found on mitotic spindles as it is in animals. The tobacco Kinesin-5, TRKP125, is expressed in a cell cycle dependent manner and is bound to the midlines of the mitotic spindle and the phragmoplast (Asada *et al.*, 1997; Barroso *et al.*, 2000). The carrot Kinesin-5 DcKRP120 is localized to the midline of the phragmoplast (Barroso *et al*., 2000). It has been proposed that Kinesin-5 motors play an important role in phragmoplast formation through microtubule-microtubule sliding (Asada *et al.*, 1997; Barroso *et al.*, 2000; Hepler *et al.*, 2002).

The Arabidopsis protein orthologous to TRKP125 is At2g28620 (Kinesin-5 C)**,** which is the plant kinesin most similar to the animal Kinesin-5 Eg5 that has been well studied. Arabidopsis Kinesin-5 C has the same function as in animals, in that it separates the spindle poles (Bannigan *et al.*, 2007). Contrary to the localization of Kinesin-5 in tobacco, Arabidopsis Kinesin-5 C is expressed throughout the cell cycle and the protein is located on every microtubule structure (Bannigan *et al.*, 2007). A conditional mutant of Arabidopsis Kinesin-5 C, *rsw7*, has the phenotype of collapsed anaphase spindles but unlike animal cells, it continues through the cell cycle after spindle collapse, possibly due to redundancy with other kinesins. Furthermore, the cortical microtubules in *rsw7* roots are disorganized during interphase, suggesting a novel function unrelated to mitosis (Bannigan *et al.*, 2007).

The Arabidopsis genome contains 4 sequences that fit into the Kinesin-5 family: At2g37420 (Kinesing-5 A), At2g36200 (Kinesn-5 B), At2g28620 (Kinesin-5 C), and At3g45850 (Kinesin-5 D) (Bannigan *et al.*, 2008) (Figure 4). Of these, Kinesin-5 A is most diverged from other members of the kinesin-5 family in Arabidopsis and is not closely related to any other Kinesin-5 that has been previously studied. Kinesin-5 B is the one most closely related to tobacco TKRP125, and Kinesin-5 C and Kinesin-5 D, which are very closely related to each other and the most similar to their animal homologue, are most closely related to the studied carrot DcKRP120 Kinesin-5 (Bannigan et al., 2008).

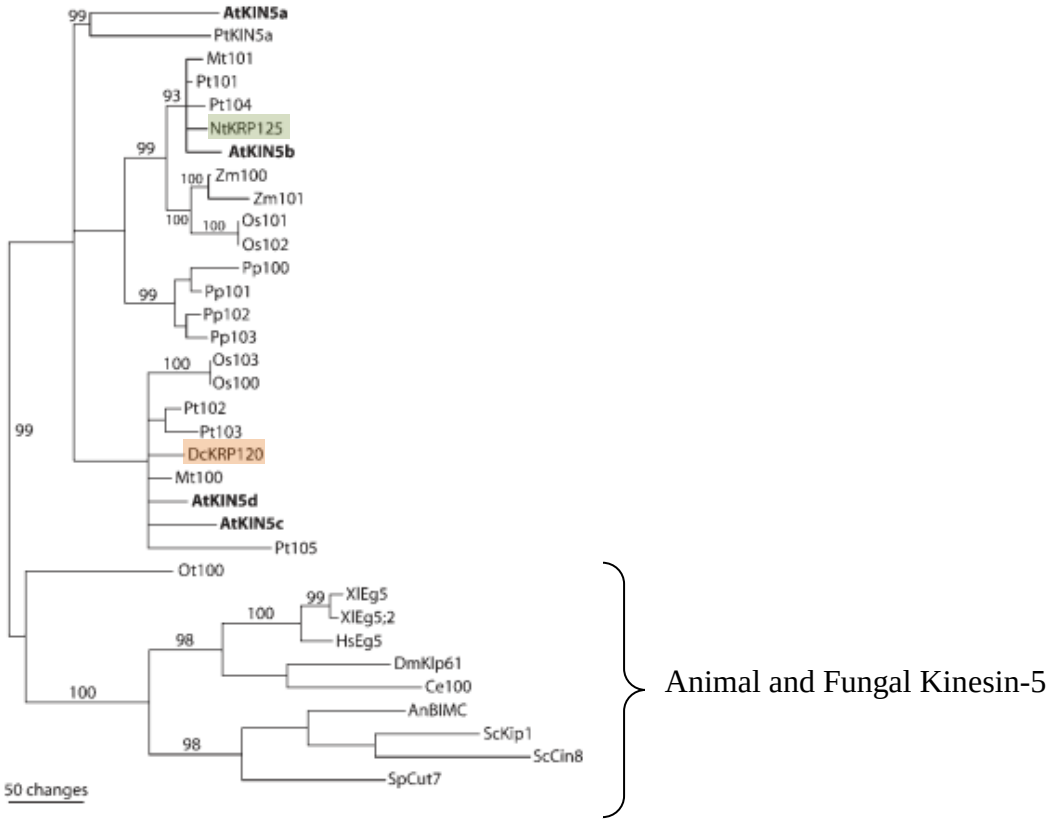

Figure 4. Phylogenetic analysis of some plant and animal kinesin-5 motor domain sequences. The tobacco gene is highlighted green and the carrot gene is highlighted orange. Species and gene names are as follows: At: *Arabidopsis thaliana* (**bold**), An: *Aspergillus nidulans*, Dc: *Daucus carota*, Dm: *Drosophila melanogaster*, Hs: *Homo sapiens*, Mt: *Medicago truncatula*, Nt: *Nicotiana tabacum*, Os: *Oryza sativa*, Ot: *Owhathehellii tauri*,Sc: *Saccharomyces cerevisae*, Sp: *Shizosaccharomyces pombe*, Xl: *Xenopus laevis*, Ce: *Cenorhabditis elegans*, Zm: *Zea mays*, Pt: *Populus trichocarpa*, Pp: *Physcomitrella patens* (Figure from Bannigan et al, 2008).

The presence of four closely related Kinesin-5 motors in the Arabidopsis genome, when many other organisms have only one or two, raises the question of their function. Do these different Kinesin-5 proteins have different specialized functions or are they simply redundant? The importance of TKRP125 and DcKRP120 in the phragmoplast suggests that their orthologs in Arabidopsis could also be important for phragmoplast structure or function. Similarly, one or more members of the family in Arabidopsis could have a specific role in the pre-prophase band. Also, considering that the *rsw7* mutant continues with mitosis unlike the animal Kinesin-5, it is possible that some aspects of the plant spindle and mitosis are unlike that of animals. Lastly, the fact that interphase microtubules are disrupted in the *rsw7* mutant opens up the possibility that, unlike in animal cells, other members of the Arabidopsis Kinesin-5 family might perform functions unrelated to mitosis.

In this study, the function of these motor proteins was investigated by examining available T-DNA insertion mutant lines in Kinesin-5 A, Kinesin-5 B and Kinesin-5 D. Cortical microtubule alignment, cell shape and mitotic array morphologies were analyzed and compared to those of the wild type. The analysis of the results suggests that Kinesin-5 A and B might be partially redundant but they do have different minor roles in different parts of the plant. Also, the results of the the Kinesin-5 D gene T-DNA insertion line screens suggest that Kinesin-5 D plays an essential, yet unknown, role.

II. Methods

Model Selection:

Arabidopsis thaliana var. Columbia was chosen as a model to study plant Kinesin-5 motor proteins because it has been sequenced completely, an extensive collection of T-DNA insertion lines are available and it is easy to grow in the laboratory. Also, the only known mutant for a plant Kinesin-5 gene, *rsw7*, is in Arabidopsis (Bannigan *et al*., 2007).

Plant Growth and Seed Collection:

Wild type and *rsw7* seeds were acquired from Tobias Baskin (University of Massachusetts, Amherst) and seeds for T-DNA insertion lines were obtained from the Arabidopsis Biological Resource Center (Ohio State University). Seeds were surface sterilized with 25 % commercial bleach for 10 minutes followed by three, five-minute rinses in sterile water. For immunofluorescence labeling, the seeds were plated on agar media containing 1 % Bacto-agar **(**BD, 214010**)** and 1 or 3 % sucrose in Hoagland's solution (4 mM KNO_3, 1 mM $Ca[NO_3]_2$, 0.3 mM $MgSO_4$, 2 mM KH_2PO_4, 89 µM Fe-EDTA, 46.2 µM H_3BO_3, 9.088 µM $MnCl_2$, 00.312 µM $CuSO_4$, 0.765 µM $ZnSO_4$, 0.153 µM MoO_4). The plates were sealed with parafilm and placed vertically under continuous fluorescent light for 6 days at room temperature (19-23^oC). For flower crossing and seed collection, plants were grown in Sunshine Mix 3 Germinating soil (Sun Gro Horticulture Inc. Bellevue, WA, USA) under a 12 hour light/dark cycle and watered once with nutrient solution (5 mM KNO_3, 2 mM $Ca[NO_3]_2$, 2 mM $MgSO_4$, 2.5 mM KH_2PO_4, 7 mM H_3BO_3, 1.4 mM $MnCl_2$, 0.05 mM $CuSO_4$, 0.1 mM $ZnSO_4$, 0.02 mM $NaMoO_4$, 1 mM NaCl, 0.001 mM $CoCl_2$). The plants were then watered as needed with tap water.

Line Crosses

To generate double mutants from T-DNA insertion lines, flowers were cross-pollinated by dissecting out the immature stamens from a flower that had a mature pistil. Pollen from another plant's mature anthers was spread onto the stigma of the emasculated flower. The resulting silique was picked when light brown. Most of the seeds were air dried and stored at 4^{o}C. Before planting, all seeds were kept at 4^{o}C for at least 24 hours.

Extracting DNA and Screening for T-DNA Insertions Using PCR

To confirm the acquired T-DNA insertion lines as carriers of the T-DNA insertion in the expected gene, PCR was performed. Leaves the size of a microcentrifuge tube cap were frozen in a tube at -80^{o}C and then crushed on ice. The powder was dissolved in 400 µl of Extraction Buffer (200 mM Tris-Cl pH 7.5, 250 mM NaCl, 25 mM EDTA, 0.5 % SDS). This slurry was spun at 13,000 rpm in table-top microcentrifuge for 10 minutes. To precipitate DNA, 300 µl of supernatant was mixed with 300 µl of 2-propanol. This was centrifuged for 10 minutes at 13,000 rpm. The pellet was washed for 5 min with 70 % ethanol, centrifuged to collect and remove remaining ethanol and then the pellet was air dried. The clean pellet was resuspended in 20 µl of TE buffer (10 mM Tris-Cl, 1 mM EDTA).

Suggested primers from the Salk Institute Genomic Analysis Laboratory were used for each of the Salk and Sail T-DNA insertion lines (Table 1). Primers were ordered from Integrated DNA Technologies.

Table 1. Primers used to screen the different T-DNA lines.

Gene name	Gene Number	Salk line number and designated working notation in ( )	Left-hand Primer 5’ to 3’	Right-hand Primer 5’ to 3’
Kinesin-5 A	At2G37420.1	Salk_055520 (A)	TGAACCTCGTTCAAGAAGAGC	ATTTGGATCTGCTTCCACTCC
Kinesin-5 B	At2G36200.1	Salk_048518c (B)	CAGACGCTTTTTCATCCTCTG	ACACAACGATGGAGCAAACTC
Kinesin-5 D	At3G45850.1	Salk_121030 (D-I)	AGAAACCACATGTTGCCAAAC	ATCAAGTTTCAGCAATGGTGG
Kinesin-5 D	At3G45850.1	Salk_025651 (D-II)	TCCAGTCACAGCTCACACAAC *	GTACAGCCATTTGGACCTACG*
Kinesin-5 D	At3G45850.1	Salk_009277c (D-III)	CAAATTGACGAGGCTCTTGAG	GTTCTGTGCGTAGCTGAAAGG
Kinesin-5 D	At3G45850.1	Sail_731_E04 (D-IV)	TATCTTTTCAGCCATTGCCTG	GAAGACGGGAAAGGAAGTGTC
Kinesin-5 D	At3g45850	Salk_025134 (D-V)	CCTTTCAGCTACGCACAGAAC*	GATCGATGGAAGTAAGGAGGC*
Left border (LB) primers that recognize the T-DNA insertion sequence: For the Salk T-DNA insertion lines: LBb1.3 5’ ATTTTGCCGATTTCGGAAC 3’ For the Sail lines : LB1 5’GCCTTTTCAGAAATGGATAAATAGCCTTGCTTCC 3’				

* The primers used to screen DII and DV T-DNA insertion lines are interchangeable i.e. both lines can be screened with both sets of primers.

Reaction mixes of three primer combinations were used to confirm the presence of a T-DNA insertion. The LP and RP primers border and amplify the gene of interest if no T-DNA insertion is present. If a T-DNA insertion is present between the LP and RP primers then the primers are too far apart to amplify anything. If the insertion is present in both copies of the gene, then this primer set gives no product. The LP primer or RP primer, which bind to the gene, in combination with either the LBb1.3 primer (for Salk lines) or the LB1 primer (for Sail lines), which bind to the T-DNA, were used to amplify either the left or right side of the gene. Either one of those sets shows a product if a T-DNA insertion is present in the gene of interest (Figure 5).

The PCR reaction mix contained 1x PCR buffer, 2mM $MgCl_2$, 0.2mM dNTP, 0.4µM of each primer and 1 unit of EconoTaq DNA Polymerase (Lucigen Catalog No 30031). The PCR protocol was 12 min at 95^{o}C + 36 x (15 sec at 94^{o}C + 15 sec at 53^{o}C annealing + 1 min at 72^{o}C) + 10 min at 72^{o}C + ∞ min 4^{o}C. The PCR products were run on 1 % Agarose electrophoresis gel for 25 minutes and stained with 5µg/ml ethidium bromide for 5 minutes. Gel images were taken using Gel Doc™ XR (BioRad).

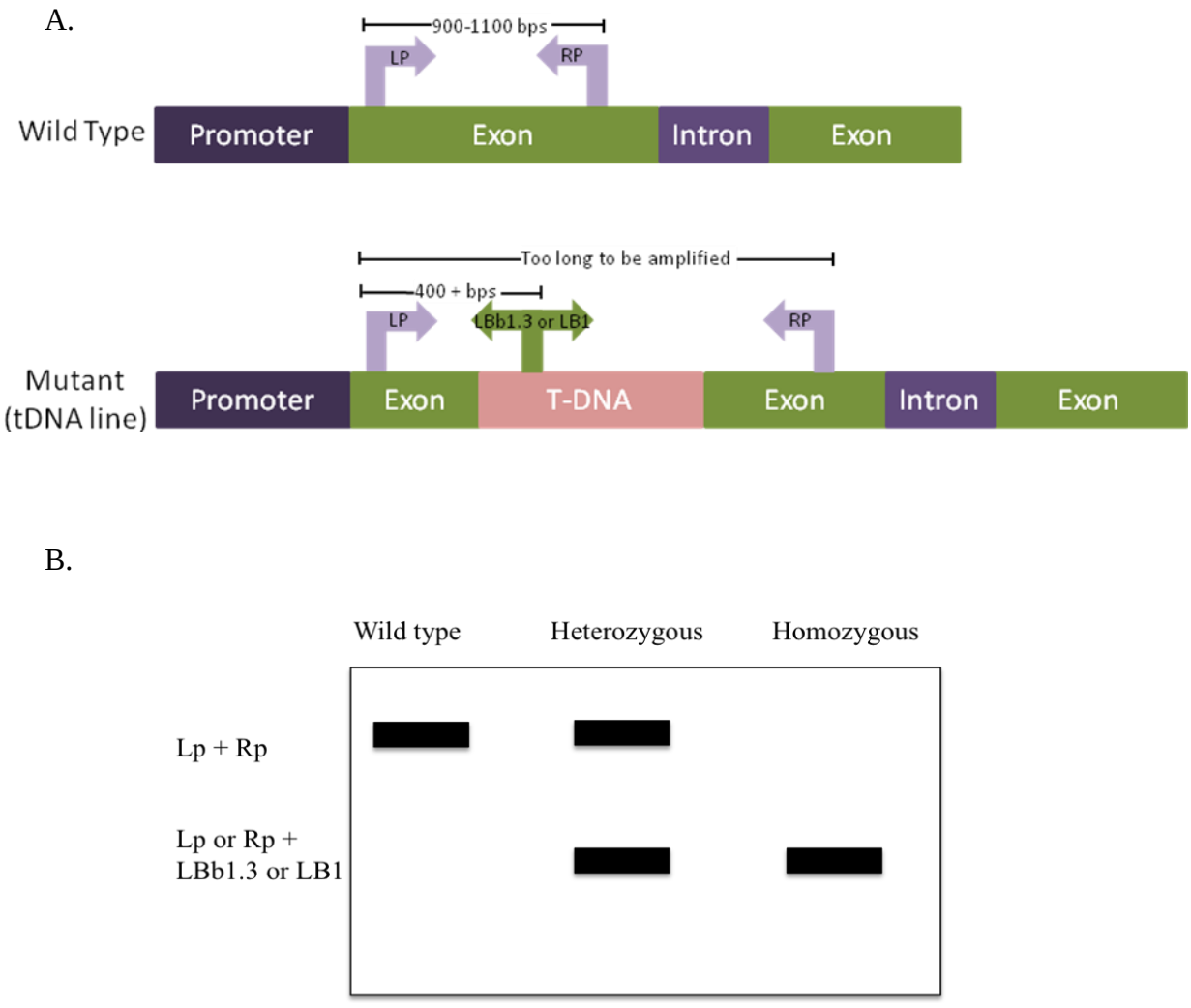

Figure 5. Illustration of the concept and steps taken to confirm T-DNA insertion lines. A. Diagram of primer combinations used for PCR screening of T-DNA lines. The primers LP and RP together amplify part of the wild type gene, but are not able to amplify the same gene if it has a T-DNA insertion. The LP or RP primers in combination with either LBb1.3 for Salk lines or LB1 for Sail lines amplify a band if there is a T-DNA insertion. B. Typical genotype result.

Gene Expression

In order to determine whether or not the gene of interest was being expressed in confirmed T-DNA insertion lines, RT-PCR was performed. A Qiagen RNeasy® Plant Mini kit (Qiagen, 74903) was used to extract RNA. Briefly, 100 mg of whole 10 day old seedlings grown in 24 hr light at 19°C was frozen in a cold mortar and pestle on dry ice. The frozen tissue was pulverized and then resuspended in the kit lysis buffer. This slurry was centrifuged through a resin column which was later washed several times. The RNA was eluted with 30 µl of water. To remove the DNA, Turbo DNA-Free kit (Ambion, AM1907) was used. Briefly, 14 µl of RNA was incubated for 30 min at 37°C with 1 µl of the reaction buffer and 1 µl of Dnase. The Dnase was deactivated with 1 µl of deactivation reagent at room temperature with shaking for 5 minutes. The supernatant was isolated. The quality of the RNA was measured using NanoDrop® ND-1000 UV-Vis Spectrophotometer with 1.5 µl of RNA sample. All RNA samples used had a 260/280 nm wavelength ratio of 2 or higher. cDNA was synthesized using iScript™ cDNA Synthesis Kit (Bio-Rad, 170-8890). To detect the gene via PCR, 1.5 to 2 µl of this cDNA was used. Primers used for the detection of the different genes are shown in Table 2. The positive control primers were for actin. PCR reactions were set up the same way as those for screening T-DNA-insertion lines.

Table 2. Primers used to check for RNA expression of Kinesin-5 A, B and D genes in the homozygous T-DNA insertion lines.

Gene name	Left Primer 5’ to 3’	Right Primer 5’ to 3’	Size of product
Kinesin-5 A	TTTGGTCCTAAGTCACAACAACGG	TGAACCTCGTTCAAGAAGAGC	447 bps
Kinesin-5 B	CAGACGCTTTTTCATCCTCTG	ACACAACGATGGAGCAAACTC	681 bps
Kinesin-5 D	CAAATTGACGAGGCTCTTGAG	GTTCTGTGCGTAGCTGAAAGG	593 bps
AtActin2	TAGTCAACAGCAACAAAGGAGAGC	GACCTTGCTGGACGTGACCTTAC	150 bps

Root Fixing and Staining

To observe cortical microtubule organization and mitotic arrays in root cells, six day old roots were fixed, either submerged on the agar growth plate or in a well with a fixing solution containing 4 % paraformaldehyde (Electron Microscopy Sciences, 15710), 1 % glutaraldehyde (Electron Microscopy Sciences, 16120), 50 mM PIPES (piperazine-N,N'-bis[2-ethanesulfonic acid]) pH7 by KOH and 1 mM $CaCl_2$ for 1 hour. The roots were rinsed with PME (50 mM PIPES, 5 mM EGTA, 2 mM $MgSO_4$) in wells 3 times for 10 minutes each. Then the roots were digested for 30 minutes at room temperature with 5 ml of digest solution (0.01 % pectolyase (MP Biomedical, 151804), 0.1 % pectinase (Fluka, 17389), 0.5x Phosphate Buffer Saline (PBS) (1.5 mM KH_2PO_4, 3.5 mM K_2HPO_4, 75 mM NaCl pH 7.2), 5 % glycerol, 0.2 % triton X-100, 25 mM PIPES, 2.5 mM EGTA, 1 mM MgSO4.) Then the roots were rinsed 3 times for 5 minutes each in a glycerol rinse (10 % glycerol and 0.2 % triton X-100 in PME). The roots were extracted with cold 100 % methanol at -15^{o}C for 15 minutes followed by rehydration in PBS 3 times for 5 minutes each. The roots were stained with 1/1000 monoclonal anti-alpha-tubulin clone B-5-1-2 (Sigma, T6074) primary antibody in a humidified chamber at 37^{o}C overnight. After rinsing 3 times for 5 minutes, the roots were incubated with 1/200 Alexafluor 488 conjugated goat anti-mouse IgG secondary antibody (Invitrogen, A11001; excitation 488 nm, emission 517 nm) for 3 hours at 37^{o}C. The roots were later washed 3 times for 5 minutes each in PBS followed by a rinse in distilled water and stained with 5 µg/ml DAPI (AnaSpec Inc, 83211) (excitation 356 nm, emission 460 nm) for 2 minutes. The DAPI was aspirated off and roots were rinsed once with distilled water followed by 3 rinses of 5 minutes duration with PBS. The roots tips were placed on slides with Antifade

mounting medium (4 % n-propyl gallate, 90 % glycerol, 10 % PBS), sealed with nail polish and stored in the dark at 4^{o}C.

Leaf Fixing and Staining

To observe microtubule organization in leaf epidermal cells, the protocols of Wasteneys *et al.,* (1997) and Barton and Overall (2010) were combined. Leaves were submerged in liquid nitrogen, broken to pieces using cold forceps and then fixed in -20^{o}C methanol with 1 % glutaraldehyde for 5 hours. After the methanol substitution, leaves were washed in 1x PBS 3 times for 5 min each and then digested in 2 % Driselase (Sigma, D8037), 0.5 % pectinase and 1 % BSA (Sigma, A7906) in 1x PBS for 10 minutes while shaking at room temperature. After the digest, the leaves were washed 3 times for 5 minutes each with 1x PBS. The leaves were incubated overnight at 37^{o}C with 1/1000 monoclonal anti-alpha-tubulin clone B-5-1-2 (Sigma, T6074) primary antibody in a humidified chamber. The next day, the leaves were rinsed 3 times for 5 minutes with 1x PBS. 1/200 Alexafluor 488 conjugated goat anti-mouse IgG secondary antibody (Invitrogen, A11001) was placed on the leaves which were incubated at 37^{o}C for 3 hours. These leaves were washed three times in 1x PBS for 5 minutes and then mounted on cover slips as described above with the abaxial surface of leaves facing toward the coverslip.

Leaf Epidermal Shape

To study the morphology of leaf epidermal pavement cells, cotyledons and leaves of various ages were cleared of chlorophyll by submerging them in 10 % glacial acetic acid in ethanol at room temperature for one hour or until the leaf was cleared. Then the leaves were mounted on slides in glycerol mounting medium.

Root Growth

To determine growth rates of the primary root, 10-15 surface sterilized seeds were grown on 10 cm Petri dishes containing a minimum of 15 ml of 3 % sucrose agar medium (recipe above). The seeds were allowed to grow for 5 days before monitoring daily growth by marking the back of the plate at the root's tip with a razor blade. Growth was measured by photographing the plates and tracing the root between two markings using the calibrated length measurement function in Nikon Elements. This allowed for measurement of the length of the root itself, and not just the shortest distance between two markings. The daily growth rate was calculated by adjusting each measurement for the number of hours between markings.

Microscopy and Image Analysis

Images were taken on a Nikon Eclipse TE2000 inverted confocal microscope. Immunofluorescently labeled samples were imaged with a 60X oil Plan Apo NA 1.4 objective. To illuminate the DAPI in stained roots the 408 nm laser was used. The emitted light from the DAPI was detected by a detector of 515/30 nm range. To image the microtubules labeled with Alexa 488, the 488 nm laser was used and fluorescence was detected with 590/50 nm detector.

Mitotic counts were made using z-series images. About 12 images of each root were taken at different focal planes through the well-stained area of the root (usually half the root) using line lambda to separate the microtubule (Alexa488) signal from the DAPI stained DNA.

The leaf epidermal cell images were taken using DIC with a 20 X NA 0.75 objective. Nikon Elements software was used to manually trace the outline of selected

cells and calculate the cell's perimeter and area. Area: perimeter ratios were calculated and averaged over all cells measured for each line.

To quantify the microtubule orientation and organization in elongating root cells, the angle measurement tool in Nikon Elements was used. Microtubules spanning at least half the width of the cell were measured. The angle between the microtubule and the long axis of the cell was measured.

Statistics

For all experiments significance was determined using a Student t-test with a p-value of 0.05 and lower considered significant. All t-tests were unequal variance and unpaired. All statistics were performed using Microsoft Excel.

III. Results

Phylogenetic Analysis

Annotated protein sequences from organisms with completed genomic sequences were gathered using a Blink BLAST (NCBI) search from the four different Arabidopsis Kinesin-5 proteins. To analyze the relationship between the different Kinesin-5 proteins in all plants, an unrooted tree was constructed using TreeView (Page, 1996).

The unrooted tree of annotated plant Kinesin-5 protein sequences shows that the plant Kinesin-5 proteins separate into three main branches labeled on Figure 6 as group A, B and C. The distribution of the plant sequences differs. Monocot sequences are only present in the B and C groups. All dicots have at least one sequence in each group. Group A contains only dicots, while group B and C have monocot and dicot plants. Group B and C have at least one sequence of Kinesin-5 from each plant from which sequences were collected.

Some of the plants from which sequences were collected, had various number of protein sequences in the different groups (Figure 6 C). For example, Arabidopsis has two sequences in the C group, sequence At-C (Kinesin-5 C, NP_180430.1) and At-D (Kinesin-5 D, NP_190171).

A.

In Tree	Protein ID
At-A	NP_850281.1
At-B	NP_181162.1
At-C	NP_180430.1
At-D	NP_190171.1
Rc-1	XP_002533001
Rc-2	XP_002532813
Rc-3	XP_002530335
Pt-1	XP_002309045
Pt-2	XP_002309420
Pt-3	XP_002299897
Pt-4	XP_002314206
Vv-1	XP_002274736
Vv-2	XP_002284615
Vv-3	XP_002276356
Sb-1	XP_002444592
Sb-2	XP_002440500
Sb-3	XP_002450083
Sb-4	XP_002442636
OsI-1	EEC84029
OsI-2	EAY96319
OsJ-1	EEE69143
OsJ-2	EEE62121

B.

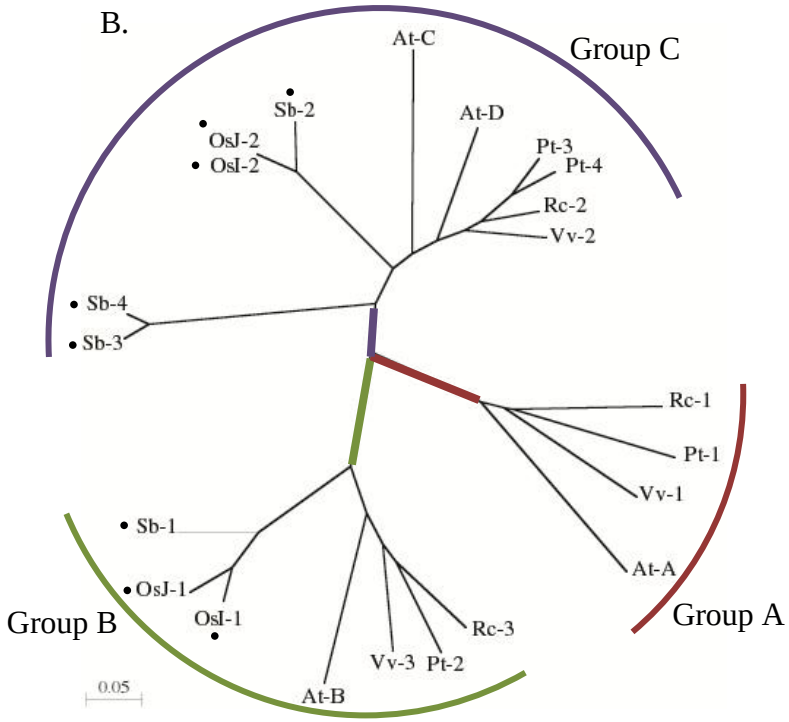

Figure 6. Unrooted tree of completely sequenced and annotated plant Kinesin-5 related proteins. A. Table of sequence ID numbers which were acquired from an NCBI protein blast of the four Arabidopsis Kinesin-5 members. B. Protein sequences were inserted into Clustal W to form an alignment which was used to make a neighbor-joining tree in Clustal W (Saitou and Nei *et al*., 1987) from which the PH file was inserted into TreeView software to form the tree shown. Black dots represent the monocots. C. Table gives distribution of plant Kinesin-5 genes of different species in the different groups.

C.

	Species	Tota	Group
At	*Arabidopsis thaliana* (thale cress)	4	A, B, C
Pt	*Populus trichocarpa* (black cottonwood)	4	A, B, C
Vv	*Vitis vinifera* (wine grape)	3	A, B, C
Rc	*Ricinus communis* (castor bean)	3	A, B, C
Sb	*Sorghum bicolor* (sorghum)	4	B, C
OsJ, I	*Oryza sativa Indica and Japonica* (rice)	2,2	B, C

T-DNA Line Confirmation

To find what the possible functions of each Kinesin-5 group might be, we obtained Arabidopsis T-DNA insertion lines (Alonso *et al*., 2003) from the SALK institute for groups A, B and D. There is already a known temperature sensitive mutant available for group C, *rsw7* (Wiedemeier *et al*., 2002; Bannigan *et al*., 2007). PCR was performed in order to select lines that contained the T-DNA insertion and were homozygous for the insertion. Some of the seeds that we received from SALK were homozygous; however, others were heterozygous. Heterozygous lines were grown to maturity and allowed to self-fertilize. The F2 seeds were collected, germinated and again screened for homozygous individuals. In some of the ordered T-DNA insertion lines, no T-DNA insertion was detected, despite numerous attempts.

The T-DNA insertion line (Salk_055520) for Kinesin-5 A (At2g37420) has an insertion in exon 1 (Figure 7A). The LP and RP primers (Figure 8) for this gene amplified a band of 1032 bp. This band was present in wild type but not in the homozygous mutant (Figure 8). The other sets of primers, LP and RP with LBb1.3, amplify a band of around 750 bp, showing that there is a T-DNA insertion. The absence of a wild-type band around 1000 bp indicates that this T-DNA line is homozygous.

The T-DNA insertion line (Salk_048518) for Kinesin-5 B (At2g36200) has an insertion in exon 17, 18 or 19, according to the information provided by the SALK Institute. The LP and RP primers (Figure 8) for this gene amplified a band of 1155 bps. This band is present in wild type but not in the homozygous mutant. The other sets of primers, LP and RP with LBb1.3, amplify a band of less than 750 bp, showing that there

is a T-DNA insertion. Two of the nine plants screened for an insertion in Kinesin-5 B were homozygous for the T-DNA insertion.

Five different T-DNA insertion lines for Kinesin-5 D: Salk_121030 (D-I), Salk_025651 (D-II), Salk_009277c (D-III), Sail_731_E04 (D-IV), Salk_025134 (D-V). To find a carrier of the T-DNA, seven plants of insertion line Salk_009277 (D-III) (Figure 7) were screened, three of which were heterozygous. These were self crossed to generate homozygous plants. The PCR screen showed that F2 plants in this line were homozygous for the insertion. The RP and LB primers gave a band size of about 1.1 kb for the wild type genome but no band for the homozygous T-DNA line. The RP and LBb1.3 showed no bands for wild type but gave a band of about 600 bp. The LP and LBb1.3 primers do not amplify a band (Figure 8).

Another Kinesin-5 D T-DNA insertion line, Sail_731_E04 (D-IV) was also homozygous, as seen in Figure 8. Out of nine plants screened three were heterozygous. These were self-crossed and F2 seeds collected and screened. The LP and RP primer amplified a band of about 1.2 kb with wild type DNA but did not amplify a band in the homozygous mutant. The LP primer with the LB1 primer showed a band a little higher above the 750 bp. The RP primer with the LB1 primer showed a band of about 750 bp for the T-DNA insertion line and none with the wild type DNA (Figure 8). This indicates that this T-DNA line of Kinesin-5 D gene is homozygous for the T-DNA insertion.

All plants screened in lines D-I, D-II and D-V were either wild type or the primers amplified ambiguous bands. Because we had other confirmed T-DNA insertion lines, these lines were not screened further and no phenotypic analyses were performed.

A.

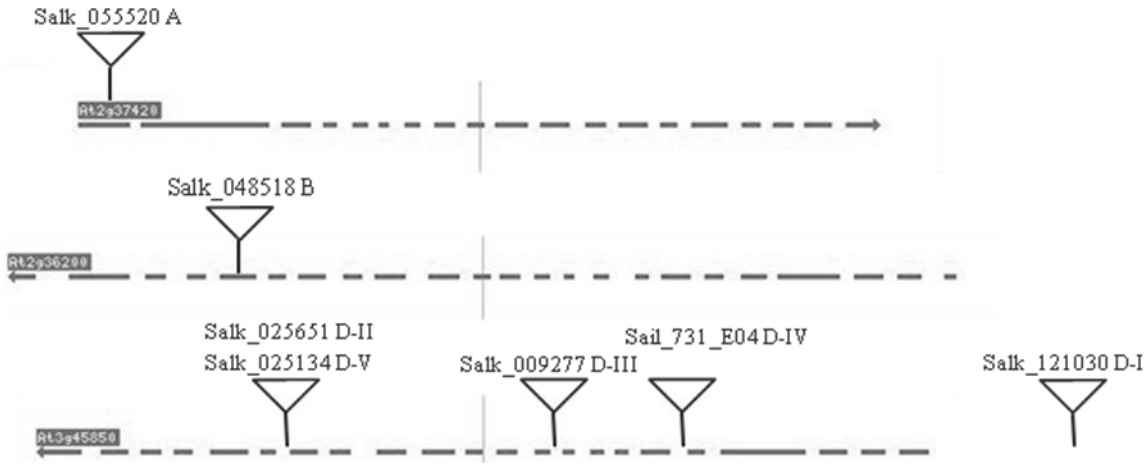

B.

Gene	T-DNA line	Position	Status
At2g37420	Salk_055520 (A)	Exon	Homozygous
At2g36200	Salk_048518 (B)	Exon	Homozygous
At3g45850	Salk_121030 (D-I)	Promotor	Wildtype
At3g45850	Salk_025651 (D-II)	Intron	Wildtype
At3g45850	Salk_009277 (D-III)	Intron	Homozygous
At3g45850	Sail_731_E04 (D-IV)	Intron	Homozygous
At3g45850	Salk_025134 (D-V)	Intron	Wildtype

Figure 7. Possible T-DNA insertion positions in the Arabidopsis Kinesin-5 genes. A. Diagram of screened Kinesin-5 A, B and D genes and the T-DNA insertion lines (Alonso *et al.*, 2003). B. Table listing the positions of the T-DNA insertions in the genes and the genotype status established through PCR screening.

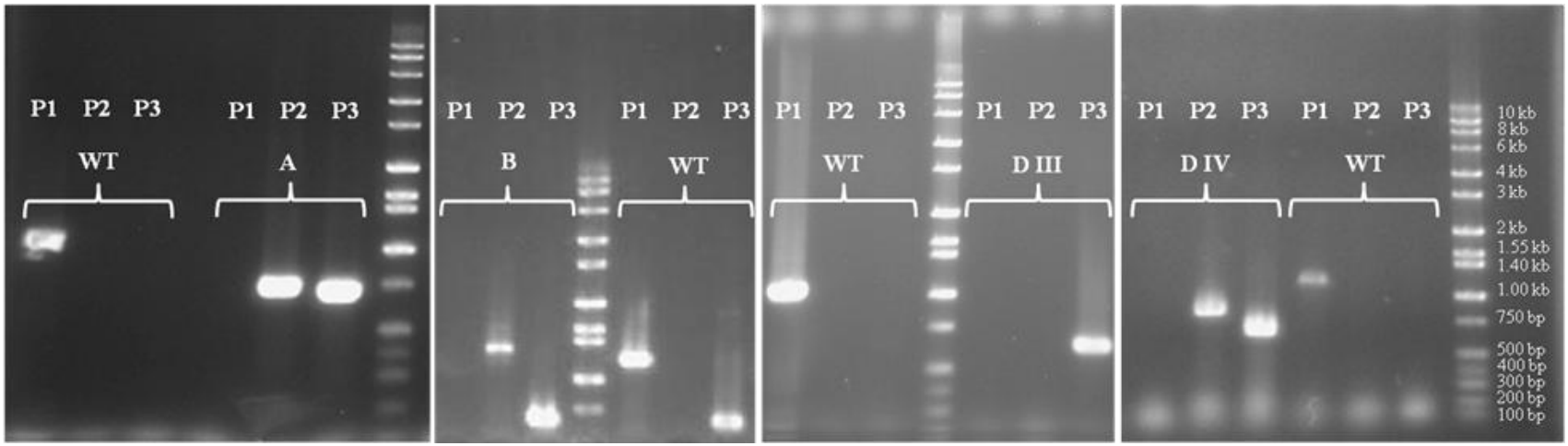

Figure 8. PCR confirmation of one or multiple homozygous T-DNA insertion lines in Kinesin-5 A, B and D genes. P1 is PCR product from specific gene primers (RP and LP). The second, P2, and third, P3, lanes are primers that amplify part of the gene and the Salk line T-DNA insertion if it is present using Lp + LBb1.3 and Rp+LBb1.3 respectively. In the P2 and P3 lanes of the Sail T-DNA line D-IV LB1 primer instead of LBb1.3 was used. Three grouped lanes (P1 to P3) are PCR products of one line; WT is wild type DNA, A is Kinesin-5A T-DNA insertion line, B is Kinesin-5B insertion line, D-III is one of the Kinesin-5D T-DNA insertion lines and D-IV is the other.

T-DNA Line Gene Expression

To see if the T-DNA insertions disrupted gene expression, we isolated RNA and checked for expression of the respective genes in the different homozygous T-DNA insertion lines for Kinesin-5 A, B, D-III and D-IV. Figure 9 shows that there was no expression of the genes of interest in the T-DNA lines for Kinesin-5 A and Kinesin-5 B. The insertion lines for Kinesin-5 D-III showed similar expression to wild type plants (Figure 9) with some unidentified band. The T-DNA insertion line for Kinesin-5 D-III shows a band just below the specific gene band. The D-IV T-DNA line shows the same expression as wild type plants. Because the T-DNA insertion lines for Kinesin-5 D all showed gene expression, they were not used for further phenotypic analysis.

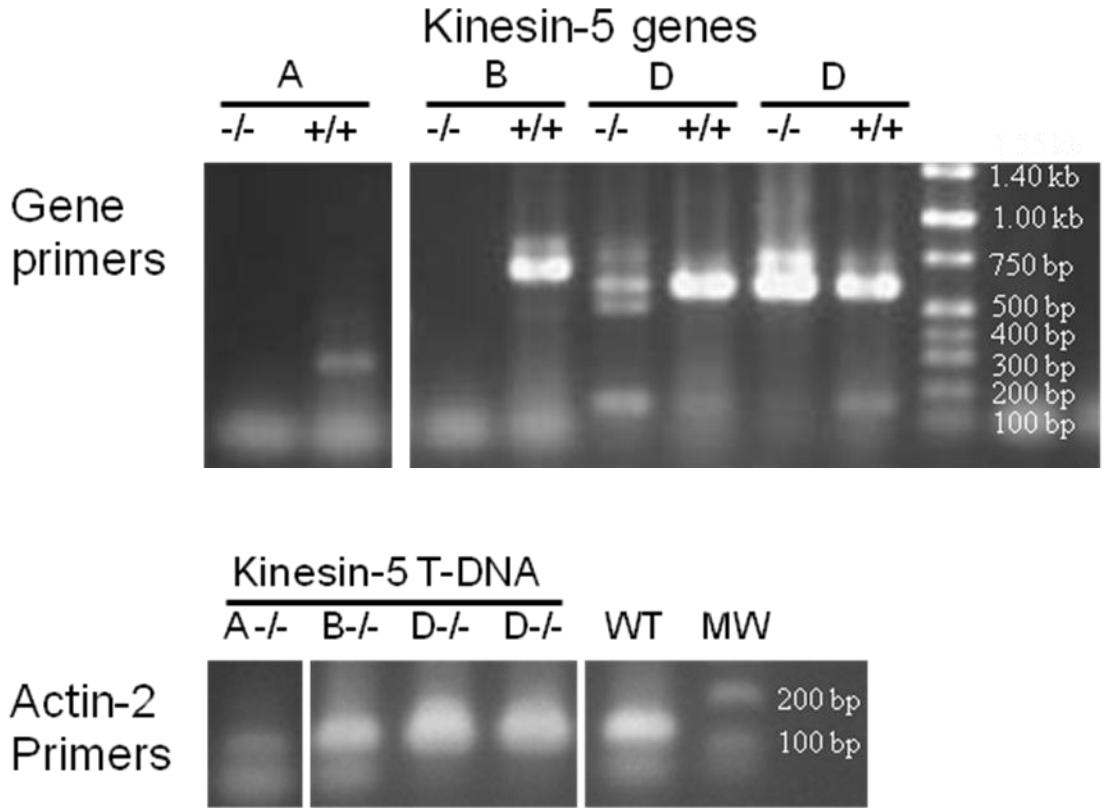

Figure 9. Messenger RNA expression of T-DNA insertion lines of Kinesin-5 A, B and D. Two T-DNA lines of Kinesin-5 D were screened. For expression control an actin primer was used. The top row identifies the gene names, Kinesin-5 A, B, and D with the genotype below it. -/- is denotes homozygous T-DNA insertion while +/+ denotes wild type.

T-DNA Line Crosses

To check for redundancy in function or co-function, single lines were crossed together in an attempt to create double and triple mutants. F2 seeds generated by crossing *rsw7* (Kinesin-5 C) with the Kinesin-5 A T-DNA insertion line and allowing the progeny to self-fertilize were screened. Out of 24 plants screened one was a double mutant. This double mutant and its progeny looked exactly like the rsw7 mutant at cellular and organ levels (data not shown).

No double mutants were found among 97 F2 plants screened from the cross between the Kinesin-5 A T-DNA insertion line and the Kinesin-5 B T-DNA insertion line.

Crosses of T-DNA insertion lines D-III and D-IV to the other lines were performed and the F2 generation was screened. Double and triple lines with *rsw7* and the Kinesin-5A T-DNA insertion line were found. However, since the expression of Kinesin-5 D was not disrupted in T-DNA insertion lines D-III and D-IV, further examination of these lines was not performed.

Mitosis

The roles of the different members of the Kinesin-5 gene family in mitosis were investigated by counting mitotic arrays in different stages in fixed and immunolabeled roots of the T-DNA mutant lines and wild type. Because it is impossible to see every cell in the Arabidopsis root tip, the number of cells in each mitotic stage was divided by the total number of mitotic cells counted in an individual root to give the proportion of cells in each stage. The T-DNA insertion mutants were compared to wild type mitotic indices. Generally, the greater the incidence of a mitotic stage, the longer that stage takes to be completed.

The stages of mitosis were identified by their chromosome arrangement and microtubule organization. Prophase was identified by the presence of a pre-prophase band and a round nucleus. Prometaphase was identified by condensed, disorganized chromosomes that did not appear to be enclosed in a nuclear membrane, lack of a pre-prophase band and a bipolar spindle around the DNA. Metaphase was identified by chromosomes aligned in the metaphase plate at the center of the bipolar spindle. In some cases, cells with good DNA staining but poor microtubule staining could be identified as metaphase by the distinctive DNA arrangement alone. Anaphase was distinguished by two separated lines of chromosomes with spindle microtubules still present at the poles. Telophase was identified by two separate DNA masses and the presence of microtubules between them, forming the earliest stage of the phragmoplast. Cytokinesis was identified by two nuclei, separated by a long narrow phragmoplast (Figure 10).

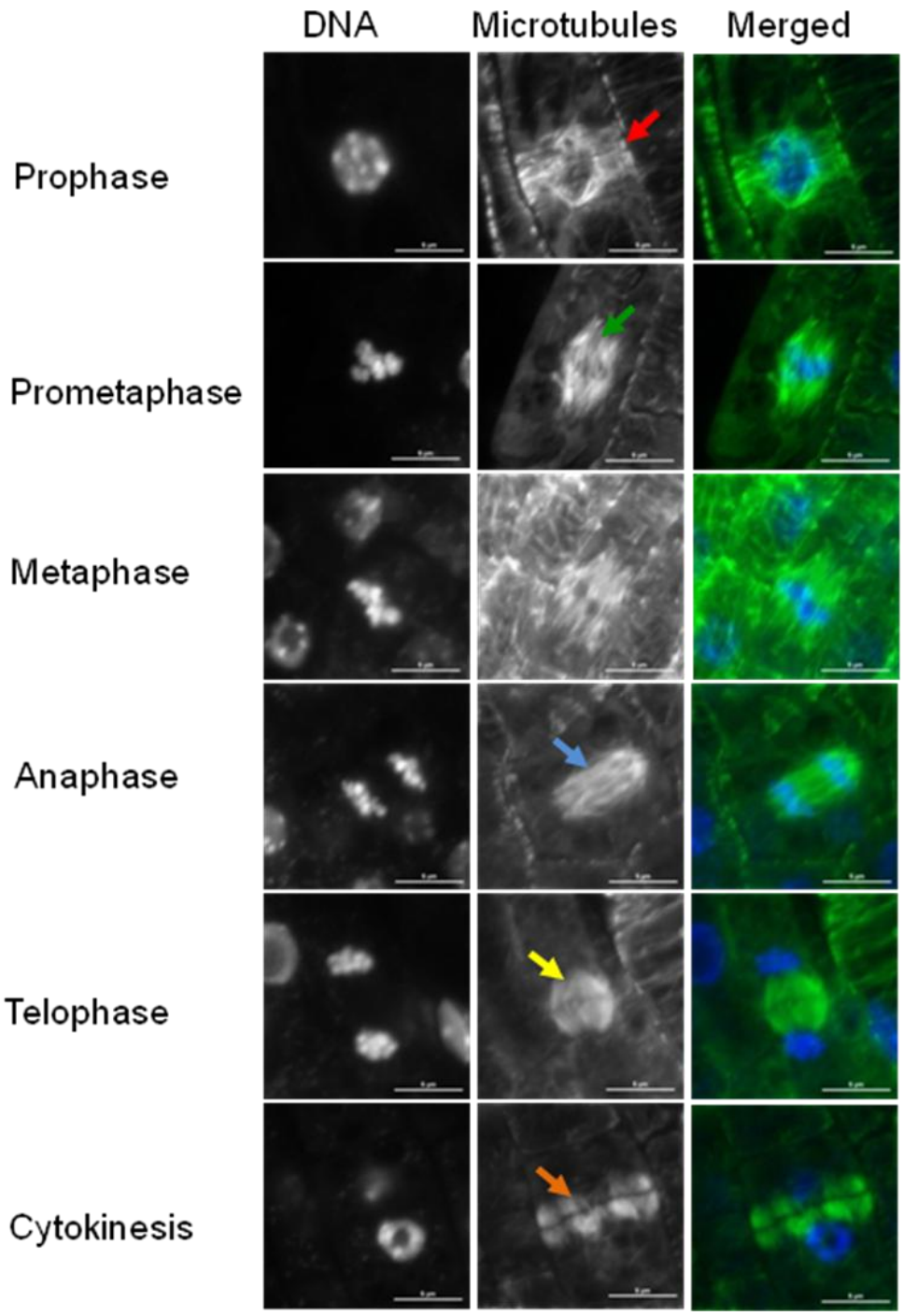

Figure 10. Confocal projection images of mitotic stages in Arabidopsis root cells. DNA was stained with DAPI and microtubules were immunolabeled with anti α-tubulin and Alexa 488. Arrows point out microtubules array used to identify the mitotic stage. Arrows are as follows: Red arrow: a pre-prophase band, green arrow: metaphase spindle, blue arrow: anaphase spindle, yellow: an infant phragmoplast, orange arrow: late phragmoplast.

In wild type plants, the percentage of cells in the stages of prophase, prometaphase, metaphase, anaphase, telophase and cytokinesis were approximately 10 %, 9 %, 39 %, 10 %, 7 %, and 22 % respectively (N=95). The Kinesin-5 A and B mutant lines showed different ratios for some mitotic phases (Figure 11).

The Kinesin-5 A mutant had an insignificantly higher percentage of mitotic cells in prophase (12 %, N=72, p-value 0.83), an insignificantly lower percentage of cells in prometaphase (7 %, p-value 0.43), a significantly lower proportion of cells in metaphase (28 %, p-value 0.016), an insignificantly lower percentage of cells in anaphase (5 %, p-value 0.21), and a significantly much higher proportion of cells in cytokinesis (39 %, p-value 0.0000001), compared to wild type.

The Kinesin-5 B mutant roots (N=57) observed also had some different proportions of cells in the various mitotic stages compared to wild type. There was a higher percentage of cells in prophase (20 %, p-vale 0. 003), about the same number of cells in prometaphase (10 %, p-value 0.57), an insignificantly lower proportion of cells in metaphase (35 %, p-value 0.27), a lower percentage of cells in anaphase (4 %, p-value 0.001), an insignificantly higher percentage of cells in telophase (9 %, p-value 0.12) and a lower percentage of cells in cytokinesis (19 %, p-value 0.40), compared to wild type.

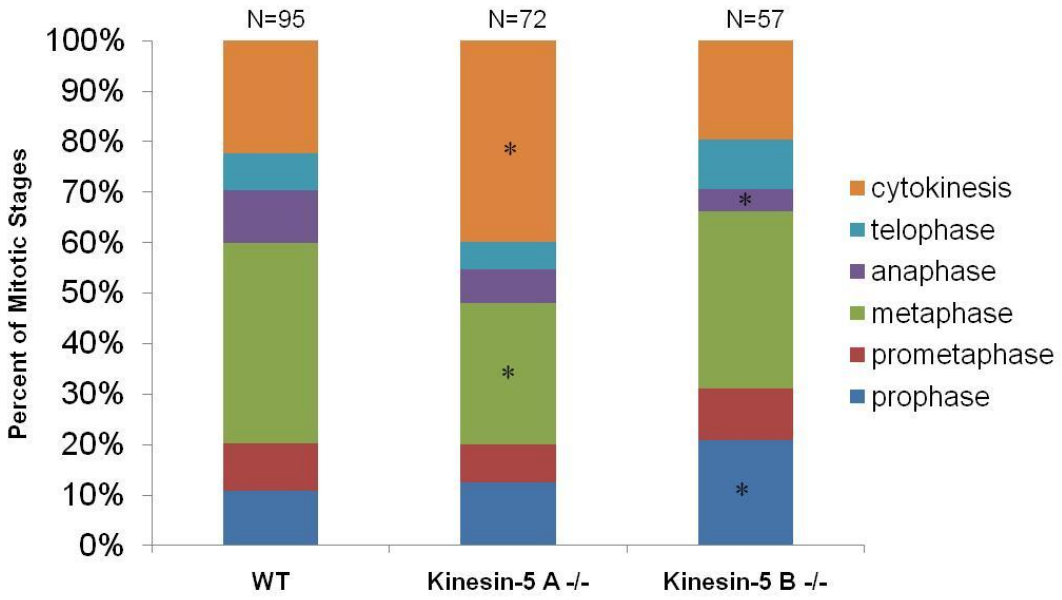

Figure 11. Mitotic stages as a proportion of total mitotic root tip cells for wild type, Kinesin-5 A and Kinesin-5 B mutants. N denotes the number of roots from which mitotic stages were counted. * indicates significant difference from wild type with p-value <0.05.

In summary, the mitosis indices significantly different at a p-value of 0.05 or lower for the different mutant lines were: lower metaphase and higher cytokinesis proportions for Kinesin-5 A mutant and a higher prophase and lower anaphase for the Kinesin-5 B mutant. Proportions reflect the duration of time each mitotic stage takes. In the Kinesin-5 A mutant because there was a lower proportion of cells in metaphase compared to wild type then metaphase happens faster than it does in wild type, while cytokinesis takes longer than it does in wild type. In the Kinesin-5 B mutant, prophase lasts longer and anaphase appears to happen faster than in the wild type.

The mitotic stages that showed significant indices (proportion) variation between wild type and mutants, prophase, metaphase and anaphase, were further analyzed to see if the index changes were the result of disrupting the structure of the mitotic microtubule arrays. The pre-prophase band width and the pole and midzone widths of metaphase and anaphase spindles were measured (Figure 12). In metaphase and anaphase cells, the width of the spindle at the poles and at the midzone was measured, and a pole to midzone ratio was calculated to compensate for different sizes of the spindles overall (Figure 12).

There was no significant difference between the average pre-prophase band widths of wild type and Kinesin-5 B mutant plants (Figure 13) (WT: 3.2 μm ±0.52, N=20, KIN5-B: 3.0 μm ±0.65 N=26, p-value 0.33) even though prophase was significantly slower in this mutant.

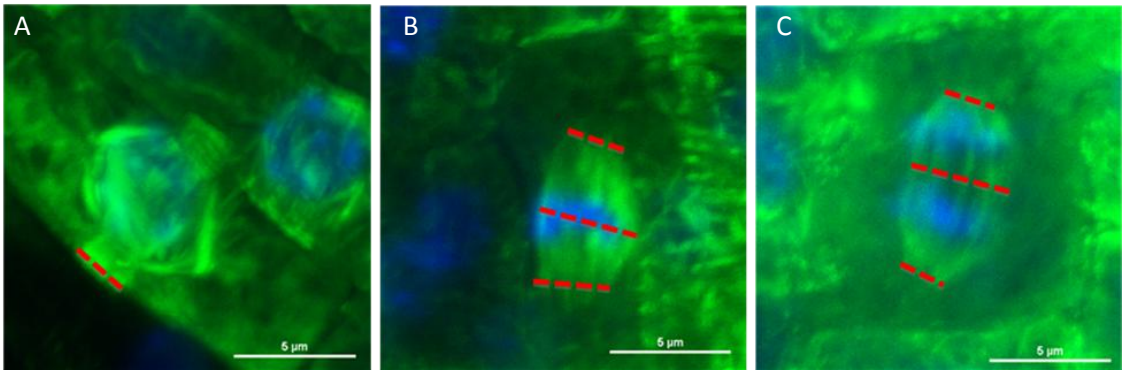

Figure 12. Mitotic stages showing measurement parameters of the microtubule arrays in the affected mitotic stage in the Kinesin-5 A and B mutants. Pre-prophase band widths (A) were measured at the most visible edge. For the metaphase spindles (B) the midzone of the spindle and the spindle poles were measured. For anaphase spindles (C), the midzone between the two nuclei was measured along with the spindle poles.

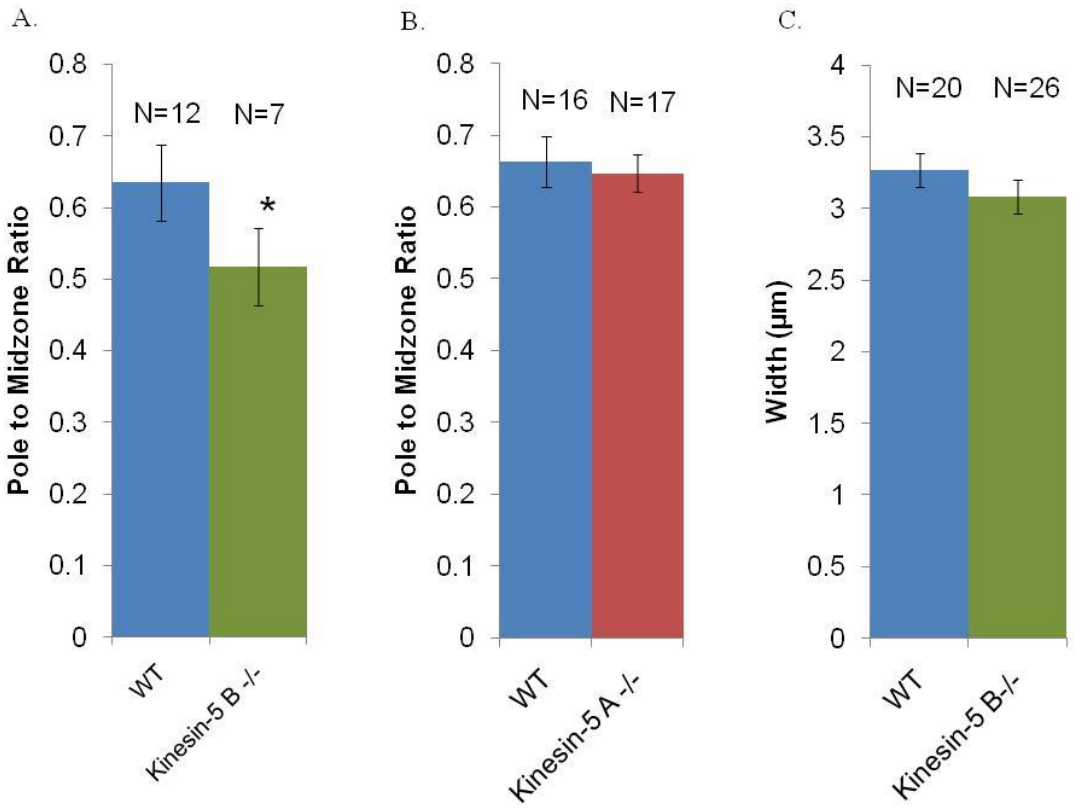

Figure 13. Measurements of microtubule arrays of affected mitotic stage in Kinesin-5 A and B mutant. A. Pre-prophase band width in wild type and Kinesin-5 B mutants. B. Pole to midzone width ratio of metaphase spindles in Kinesin-5 A mutant and wild type. C. Pole to midzone width ratio of anaphase spindles in Kinesin-5 B mutant compared to wild type. Bars indicate ± Standard Error. N denotes the number of cells measures. *indicates significant difference with p-value of <0.05

In the case of the Kinesin-5 A mutant, the metaphase spindles showed no difference in pole width (WT: 0.66 μm ±0.14, N=16; KIN5-A: 0.64 μm ±0.10 N=17, p-value 0.61). In contrast, there was significant difference in the ratio of anaphase spindle pole to midzone width in the Kinesin-5 B mutant compared to the wild type (WT: 0.63 ±0.18, N=12; KIN5-B: 0.51± 0.14 N=7, p-value 0.03) (Figure 13). The poles were less broad relative to the midline in the mutant. This result is statistically significant using the student t-test, but because of the very low number of anaphase spindles that were seen in the Kinesin-5 B mutant, the sample size was very small.

The Kinesin-5 A mutant showed a higher proportion of phragmoplasts, indicating that this mutant is slowed in cytokinesis. Because the phragmoplast changes both width and length in a normally diving cell, and there is no other marker to indicate its stage, it was decided that measurements of phragmoplast would not be informative.

Root Elongation and Cortical Microtubules

We looked for interphase microtubule abnormalities of the knock-out T-DNA lines for Kinesin-5 A and Kinesin-5 B by measuring root growth rate and cortical microtubule organization. Root growth rates of the Kinesin-5 A T-DNA insertion line were similar to wild type growth rates (Figure 14). The roots of the Kinesin-5 B T-DNA insertion line showed a slightly higher growth rate. Day-by-day comparison showed that this was significant after 6 days of growth, when the wild type growth rate starts to level off.

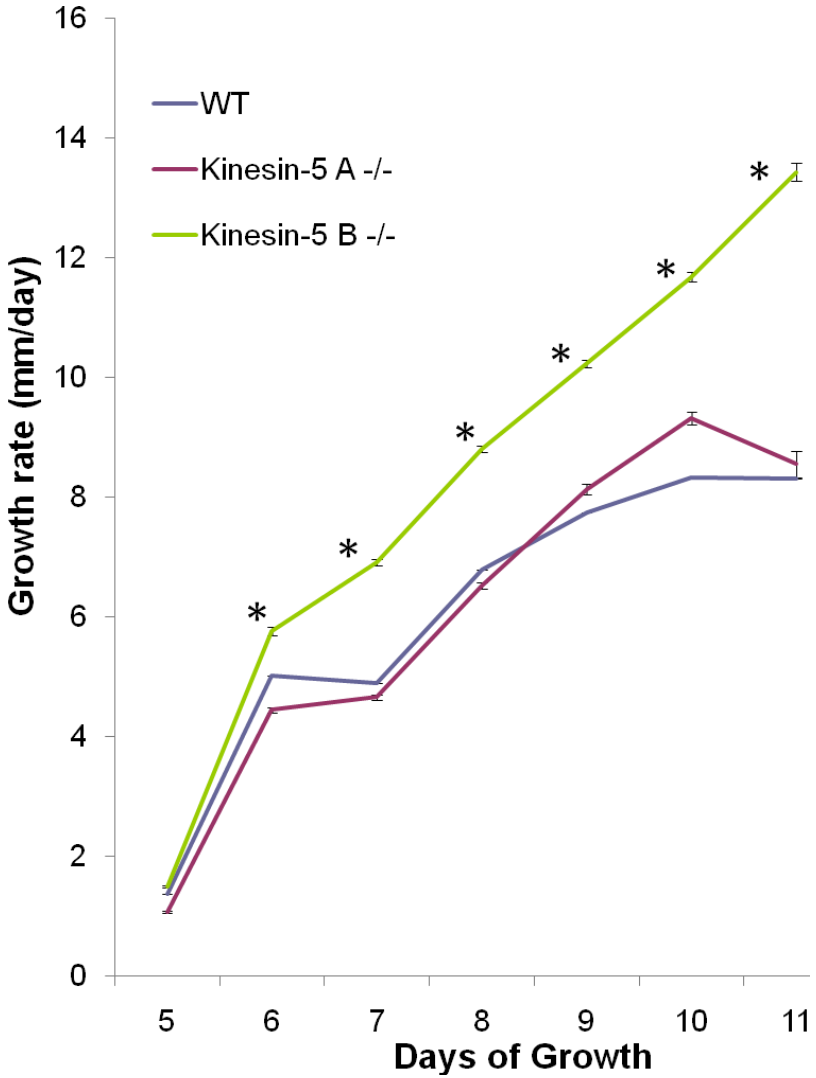

Figure 14. Root growth rates of Kinesin-5 T-DNA insertion line and wild type roots. This graph shows a typical experiment with averages from thirty seeds for each T-DNA insertion line. Error bars are ± Standard Error. * Shows the days when the growth rate of Kinesin-5 B mutant were different from the wild type growth rate.

The growth rate of roots is a function of both cell division and cell elongation and both of which are reliant on proper microtubule organization and dynamics. To further examine the effect of Kinesin-5 A and B on cortical microtubules we observed cortical microtubules in elongating root cells. The microtubules in elongating root cells appeared generally similar, and their degree of organization was difficult to judge objectively. We analyzed them quantitatively by measuring the angle of each indivual microtuble relative to the long axis of the root (Figure 15). An angle of 90 degrees represents a perfectly transverse microtubule. The range of angles represents the degree of organization of the microtubules (i.e. how parallel they are to each other).

Microtubules of eight cells from six different roots of the wild type plant gave an average orientation of 87.4 degrees (SE ± 1.66), which was not significantly different from the measurements from 11 cells from seven roots of the Kinesin-5 A mutant (Mean=87.8 ±SE 1.44) or the Kinesin-5 B mutant's 10 cells from seven roots (mean=87.5 ±1.08). The range of angle sizes within each line was not significantly different (WT: 39.3 SE ± 6; KIN5A: 39.9 SE ± 4.7 p-value 0.9; KIN5B: 28.7 SE ±.16 p-value 0.16). Cortical microtubules in the Kinesin-5 B mutant had the smallest range of angle sizes, meaning that this mutant has the most organized/ parallel microtubules compared to the microtubules of the wild type. Figure 15 shows the region from which the microtubules were measured.

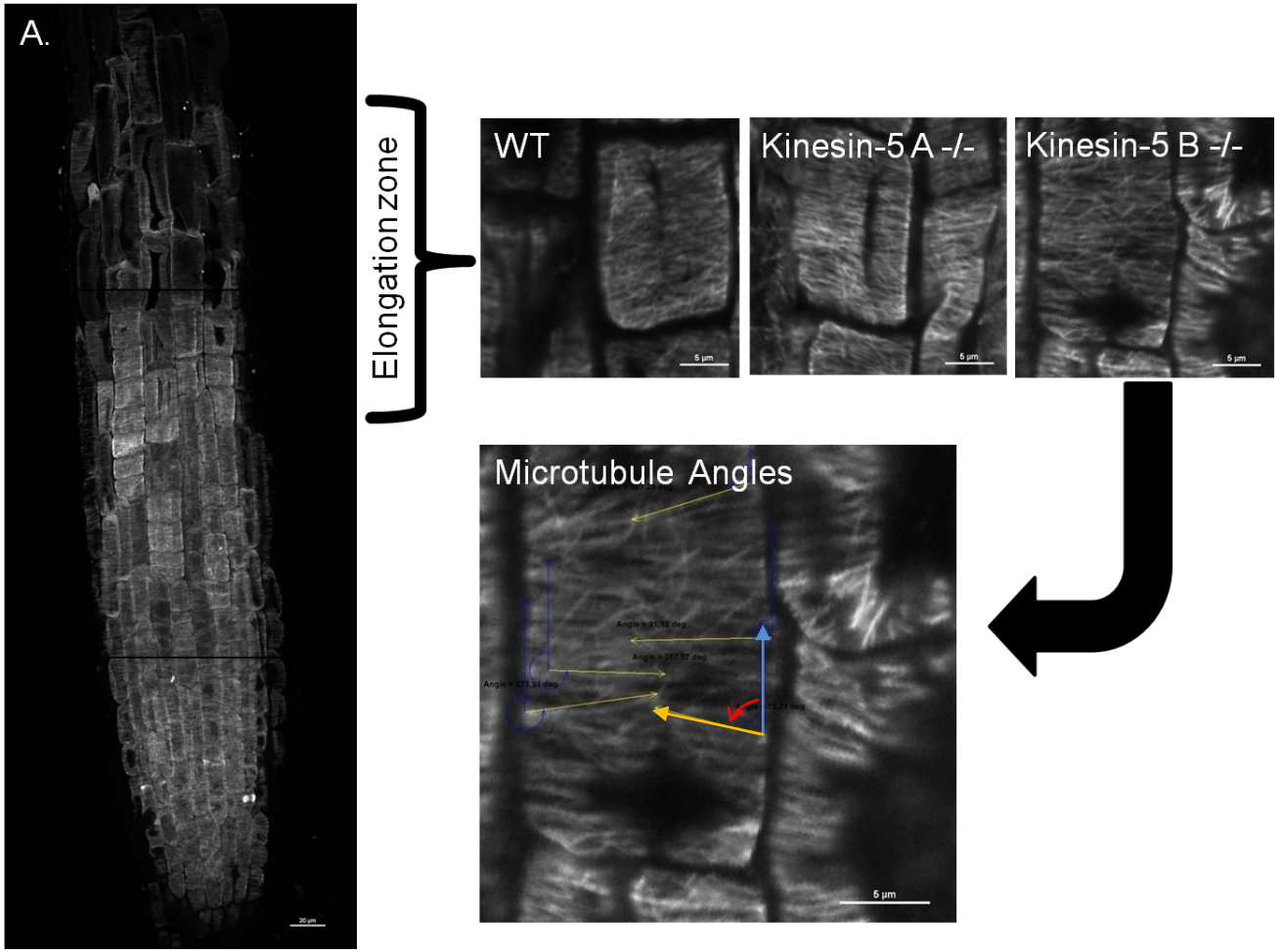

Figure 15. Confocal images of cortical microtubules in elongating root cells. A. Stitched micrographs of confocal projections of a wild type root immunolabeled for alpha tubulin. B. Cortical microtubules in wild type and the Kinesin-5 A and B mutants from the elongating region of roots. C. Example of how angle measurements were taken to calculate orientation and organization.

Specialized Cell Shapes

The trichome morphology of the Kinesin-5 A and Kinesin-5 B T-DNA mutants was not obviously different from wild type. In all lines, the trichomes had a short pedestal which separated into three straight, slender branches at the apex (Figure 16). Size and distribution of trichomes on the leaf surface appeared to be similar in the mutant lines and the wild type.

Mature rosette leaves were observed to investigate possible cell shape defects in epidermal pavement cells in Kinesin-5 A and B mutants. During normal leaf development, the shape of the pavement cells varies in the different areas of the leaf. With that in mind, images of pavement cells were taken from just the medial lateral area of the leaves for consistency (Figure 17). Perimeters of visible pavement cells were measured. The area to perimeter ratio was calculated to compare the lobe formations of the wild type (mean=6.20, N=31) and the mutant Kinesin-5 lines. The Kinesin-5 B mutant showed no difference in pavement cell shape compared to the wild type cells (mean=6.42, N=19, p-value=0.18). The Kinesin-5 A mutant had less convoluted margins, which are represented by a significantly higher area to perimeter ratio (mean=7.08, N=31,P-value= 0.000008), indicating reduced lobe formation and indentation (Figure 18).

To better analyze the influence of Kinesin-5 A on microtubules of pavement cells, pavement cells were labeled for alpha-tubulin. Stained cells at the cut edge of the leaf were imaged because they were the ones stained. The microtubules in the wild type leaf epidermal cell and those of the mutant Kinesin-5 A did not show an obvious difference in organization (Figure 19).

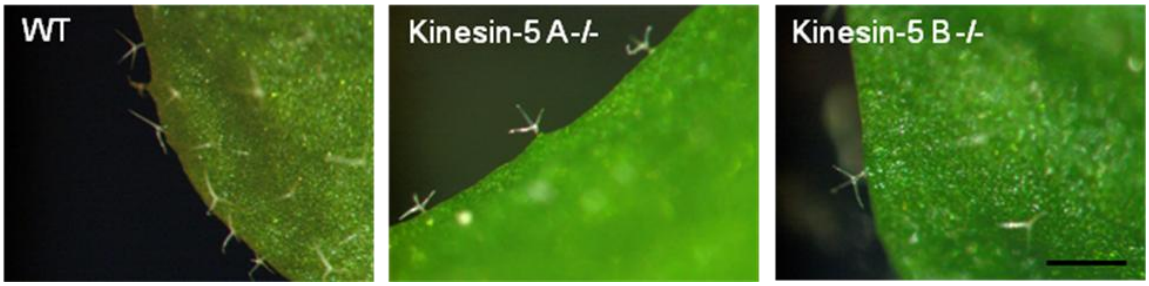

Figure 16. Images of multiple trichomes on mature leaves. Trichomes have three branches and look normal in both of the Kinesin-5 mutant lines. Scale bar = 400 µm.

A.

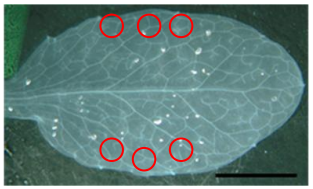

B.

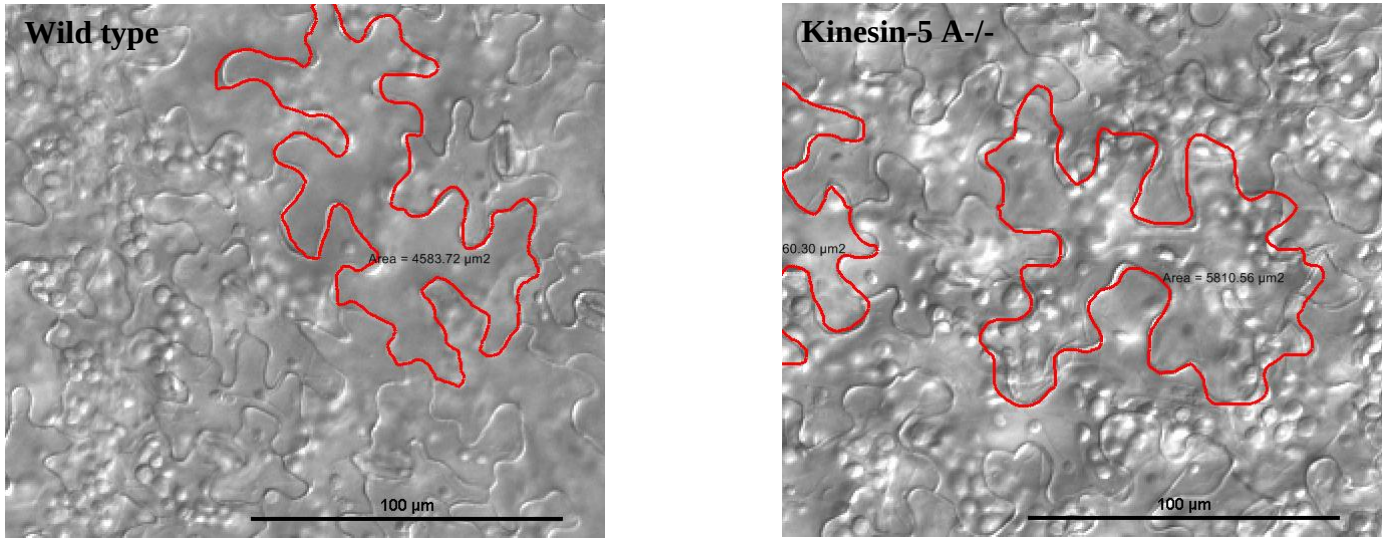

Figure 17. Leaf pavement cell shape. A. Whole leaf with marked areas (red circles) where images of pavement cells were taken for measurement. Bar is 0.5 cm. B. DIC images of cleared leaves from a wild type leaf and Kinesin-5 A mutant. Bar is 100 µm.

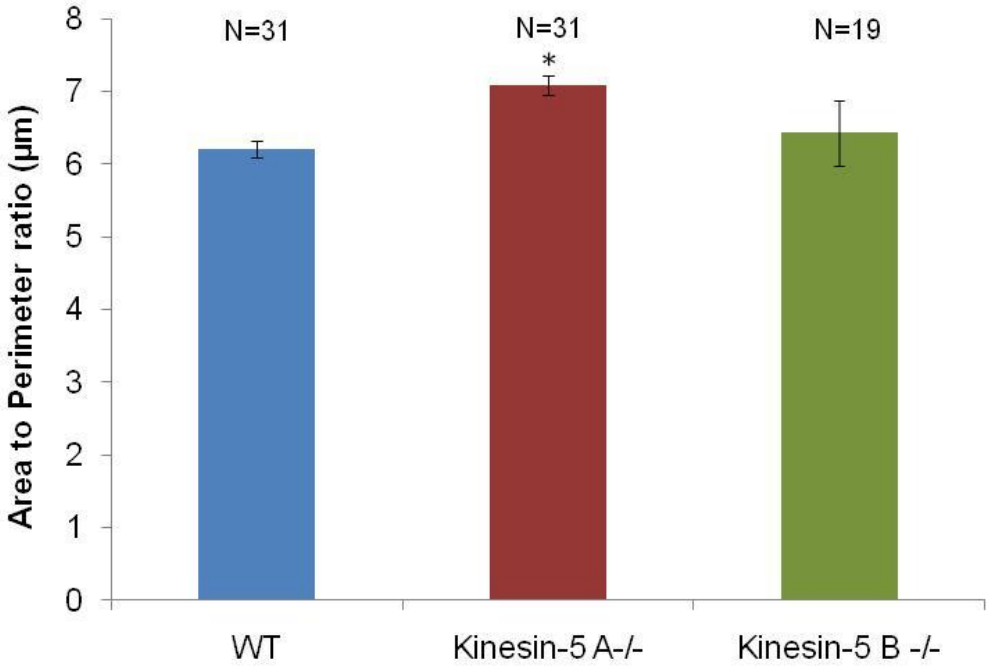

Figure 18. Average area to perimeter ratio of wild type, and Kinesin-5 A and Kinesin-5 B mutant pavement cells. Bars are ± SE, N gives the number of cells measured and * denotes significant difference from wild type (p-value <0.05).

A.

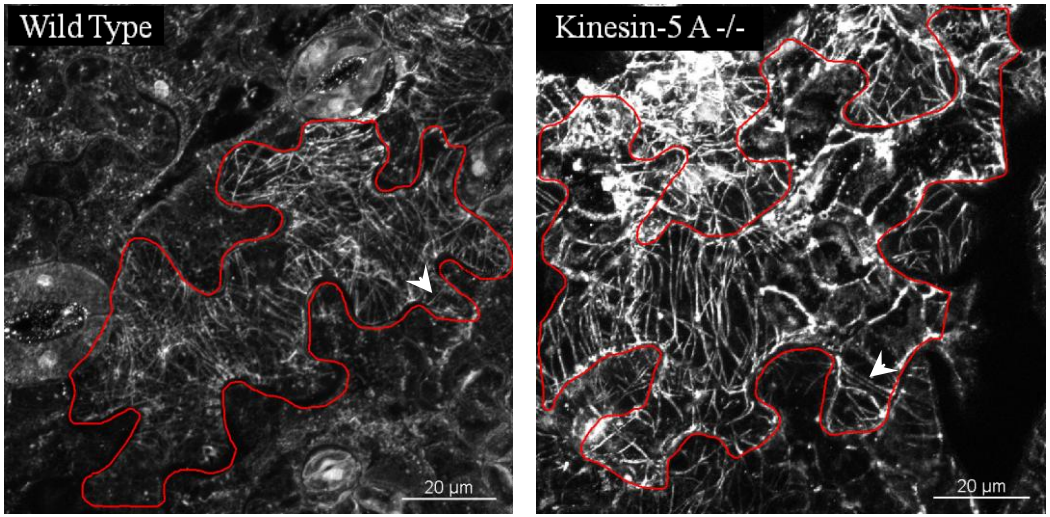

B.

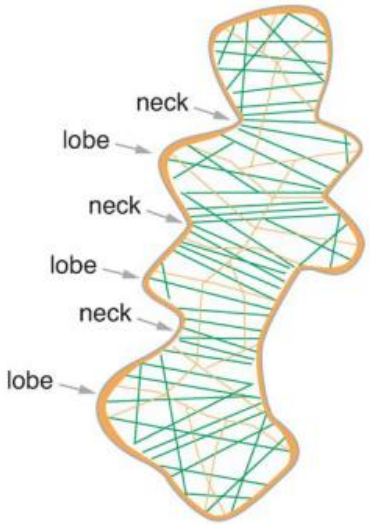

Figure 19. A. Projection of confocal images of pavement cells from wild type and the Kinesin-5 A mutant fixed and immunolabeled for microtubules. Arrows points to microtubule bundles in the neck of the pavement cells. Scale bar = 20 µm. B. Illustration of expanding pavement cell with microtubule (green) bundles in the neck region and actin (orange) in the lobe areas (illustration from Smith and Oppenheimer, 2005).

IV. Discussion.

The unusually large number of Kinesin-5 family members in Arabidopsis compared to animals hints at divergence amongst kinesins and specialization for functions that are unique to plant cells. In light of the lack of dynein in plants (Lawrence *et al*., 2001), the existence of microtubule arrays in plants that are not seen in animal cells (Lloyd and Chan, 2006), as well as the intimate involvement of microtubules in the construction of the cell wall (Zhang *et al*., 1990) offer two obvious possibilities for novel Kinesin-5 functions in plants.

Of the four members of the Kinesin-5 family in Arabidopsis, Kinesin-5 C has previously been shown to be essential for mitosis, in much the same way as its homologues (Eg5, BIMC, KIF11 etc) are in animal and fungal cells (Bannigan *et al*., 2007). With this traditional role performed, at least in large part, by Kinesin-5 C, the question of the functions of the other three members of the family remains open.

Phylogenetics

The unrooted tree (Figure 6) shows that many plants have more than one Kinesin-5 member in their genome, which indicates that they are probably needed for normal cell function. It could be that these additional kinesins in plants play a role in plant-specific mitotic arrays, like the pre-prophase band and phragmoplast or there could be a redundancy in function. The grouping of two of the Arabidopsis sequences into group C indicates that they are closely related. Most plants in the tree have a gene in groups B and C, suggesting that members of group B and C are particularly important in plants and are probably not redundant. In group C, given that sequences from the other plant species are more closely related to the Arabidopsis Kinesin-5 D gene than to the Kinesin-5 C gene,

one would expect Kinesin-5 D to be at least as important as Kinesin-5 C. The Arabidopsis Kinesin-5 family members most closely related to all animal Kinesin-5 sequences also fall into group C (Figure 4), further solidifying the idea that group C kinesins are crucial for survival.

The fact that not all plants have members in group A suggests that the Kinesin-5 proteins that fall into group A in dicots might be redundant with members of either of the groups B or C. It might also be that group A members in docots perform a function specific to dicots that is not necessary in monocots.

T-DNA Insertion Lines

Other evidence that points to the importance of group C is that a knockout mutant of Kinesin-5 C is embryo lethal (Bannigan *et al*., 2007). Also, after attempting to screen five different T-DNA insertion lines for the other Arabidopsis group C member, Kinesin-5 D, no mutants that disrupted gene expression were found, which suggests that both members of group C are essential.

The fact that both members of group C in Arabidopsis appear to be essential indicates that there might not be a redundancy in function between them, despite their high degree (85.5 %) of sequence similarity (Bannigan *et al*., 2007). It could be that they function separately in equally crucial processes or that they work together to form a functioning unit to carry out necessary processes.

Arabidopsis Kinesin-5 C is essential for the completion of mitosis (Bannigan *et al.*, 2007) and so it is lethal when completely knocked out. One possible function of the closely related Kinesin-5 D is that it might be involved in another cell division process, meiosis. To investigate this, pollen and ovule morphology and pollen germination rate

could be examined. Alternatively, if Kinesin-5 D performs an essential role other than meiosis, then knocking it out might result in embryo or seedling lethality. To test this, the siliques of heterozygous lines for Kinesin-5 D could be examined for embryo arrest or seed abortion, and seed germination assays could be performed to check embryo development and survival rates.

Kinesin-5 motor proteins are known to be homotetramers in animals: four identical subunits, each comprising a motor domain and stalk, combine to make one functional motor protein (Cole *et al.*, 1994; figure 3). Considering that the Kinesin-5 C and Kinesin-5 D are so closely related (Bannigan *et al*., 2007) it might that they interact to form a heterotetramer. In this case, the absence of either one would result in failure of mitosis. This role could be investigated by an *in vitro* binding assay. The Kinesin-5 C gene is already cloned (Bannigan *et al*., 2007) but Kinesin-5 D is not. Attempts were made to clone the Kinesin-5 D gene for this study without success (results not shown).

The screening of T-DNA insertion lines in Kinesin-5 A and Kinesin-5 B identified one mutant line for each that did not express the relevant gene at a detectable level. These single lines were further examined for phenotypic anomalies. The T-DNA lines for Kinesin-5 A and Kinesin-5 B were crossed in an attempt to make a double mutant, but without success. This could mean that Kinesin-5 A and Kinesin-5 B are redundant or compensatory in function. However, the analysis of the single lines reveals that they probably influence separate processes, at least in mature plants. As discussed below, during mitosis, Kinesin-5 A seems to play a role in metaphase and cytokinesis, while Kinesin-5 B contributes somehow to the pre-prophase band and anaphase. This means that, if both Kinesin-5 A and Kinesin-5 B are knocked out, every stage of mitosis

could potentially be disrupted, which might cause embryo lethality. This could explain the failure to isolate any double mutants of Kinesin-5 A and B, while single mutants were not detrimental because the remaining kinesin performed its function.

Mitosis Phenotypes

Cells of the root elongation zones in the different Kinesin-5 mutants were similar in shape and size to those in the wild type. There were no obvious cell division morphology or expansion defects and the overall architecture of the root appeared normal in the mutants (Figure 15).

In mitosis, differences in the proportion of cells in each mitotic stage in the Kinesin-5 A and Kinesin-5 B mutants compared to wild type are suggestive of abnormalities in the organization or function of the microtubules. However, no obvious morphological abnormalities were seen in the microtubule arrays that could explain the differences in mitotic indices observed, which points to changes in microtubule stability and dynamics as the likely effects of the mutations.

The shorter metaphase duration in the Kinesin-5 A mutant without a visible difference in spindle structure implies that Kinesin-5 A somehow affects movement, but not arrangement, of the spindle microtubules. In the Arabidopsis Kinesin-14 mutants ATK1 and ATK5, a mild spindle phenotype is coupled with prolonged mitosis (Marcus et al., 2003; Ambrose et al., 2005; Ambrose and Cyr, 2007), which demonstrates that kinesins in the spindle affecting the cell's progress through mitosis. During metaphase Kinesin-5 A probably cross links microtubules and so stabilizes the metaphase spindle (figure 20).

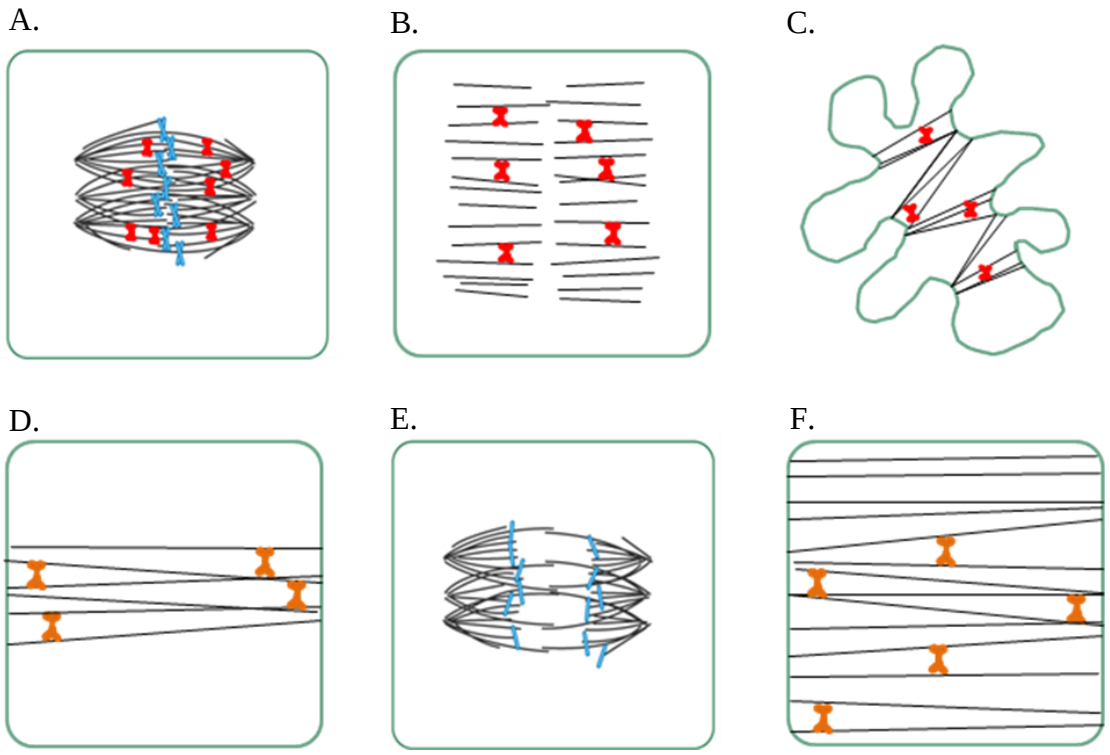

Figure 20. Illustrations of proposed roles of Kinesin-5 A (red) and Kinesin-5 B (orange) motor proteins in the different mitotic arrays and interphase microtubules. A. metaphase spindle with chromosomes (blue) attached to microtubules (black). Kinesin-5 A cross links the metaphase spindle microtubules restricting movement. B. Phragmoplast with Kinesin-5 A cross linking individual microtubules and stabilizing the array. C. Pavement cell with microtubule bundles showing (black) and Kinesin-5 A bundling the microtubules by cross linking them. D. Cell during prophase with pre-prophase band. Microtubule dynamics is affected by the presence of Kinesin-5 B so that the pre-prophase band disassembles faster. E. Anaphase spindle with Kinesin-5 B in the midzone restricting the movement of the microtubules. F. Kinesin-5 B attached to cortical microtubules and increasing the dynamics resulting in a less parallel cortical array. The metaphase and anaphase images were modified from Bannigan *et al*., 2007.

Without Kinesin-5 A metaphase completes faster because there is no cross linking to resist the movements of other motors. To further analyze this mutant it could be crossed to a plant expressing GFP-tubulin to visualize the mitotic spindle in live plants as it forms and as it separates the chromosomes. Live cell imaging of GFP-tubulin labeled mutant mitotic cells would show how the spindle is assembled and moves compared to the wild type.

The delay in completing cytokinesis in the Kinesin-5 A mutant suggests a defect in either cell wall synthesis or the stability of the phragmoplast microtubules, but unlike the Kinesin-5 C mutant, *rsw7,* which has a severe wall placement defect (Bannigan et al., 2007), the walls of the Kinesin-5 A mutant appeared normal. So, it is likely that the phragmoplast stability is influenced by the mutation, not wall synthesis. When the phragmoplast is forming Kinesin-5 A could cross link microtubules and stabilize them (figure 20). Without Kinesin-5 A the phragmoplast becomes unstable and so more time is needed for building the new cell wall.

The Kinesin-5 B mutant showed two seemingly contradictory phenotypes in mitosis: slowed progression through prophase and a faster completion of anaphase. It is well established from animal and fungal studies that the dynamics of the spindle rely not on the action of any single motor protein, but on the balance of forces exerted by many different motors (Sharp et al., 2000). This is likely to be the case in plants also (Bannigan et al., 2008). Kinesin-5 B might be involved in anchoring spindle microtubules to each other in the anaphase spindle and slowing movement by opposing other motor proteins similarly to the *Caenorhabditis elegans* Kinesin-5, BMK-1, which resists pole separation

in elongated anaphase spindles (Saunders *et al*., 2007). There were no collapsed spindles in the Kinesin-5 B mutant like those seen *rsw7* (Bannigan et al., 2007), suggesting that this motor is probably not a major force generator during spindle movement but rather restricts the movements caused by the other motors. The opposing force that the Kinesin-5 B motor provides might be slight and so when it is not present the other motors work with slightly less opposition, resulting in faster anaphase (Hentrich and Surrey, 2010).

When looking at the anaphase spindle in the Kinesin-5 B mutant, it was observed that the poles of the spindle were narrower than those in wild type cells. The spindle shape overall were not visibly different from wild type in the Kinesin-5 mutants, unlike *rsw7*, which has collapsed spindles (Bannigan et al., 2007), or Kinesin-14 motor mutant, *atk-5*, which has obviously elongated, bent spindles and splayed poles (Ambrose and Cyr, 2007). This might also be indicative of its minor role in force generation during spindle elongation.

In the pre-prophase band, Kinesin-5 B protein might function in the assembly or disassembly of the pre-prophase band by influencing the polymerization and depolymerization of microtubules. Kinesin-5B could increase microtubule dynamics, which means it increases the rate of polymerization and depolymerization (figure 20). Considering that the pre-prophase band is formed by the changing dynamics of the microtubules (Müller *et al.,* 2009), without Kinesin-5 B, the pre-prophase band would be less able to disassemble and therefore last longer.

Cortical Microtubules and Root Elongation

In animal cells, the only known functions of Kinesin-5 proteins are in the spindle. However, a potential role for Kinesin-5 motors in organizing the interphase microtubules in plants was revealed by the Kinesin-5 mutant *rsw7* (Bannigan *et al*., 2007). Other kinds of kinesins are known to affect cortical microtubule organization as well (Buschmann and Lloyd, 2008). Because cortical microtubule organization affects the direction of cell expansion in plants and because roots tend to elongate in one predictable direction, measuring root elongation rate is often used to identify microtubule organization anomalies (Beemster and Baskin, 1998; Wasteneys and Ambrose, 2009). Microtubules of elongating root cells are generally parallel to each other and perpendicular to the axis of root growth. The zone of elongation contains cells that transition from square to rectangular as they elongate and so the region is easy to identify visually. When the normal organization of cortical microtubules is disrupted, cell expansion loses its directionality, causing the cells to swell, and the elongation rate to decrease (Baskin *et al*., 1999).

In this study, while the growth rate of Kinesin-5 A mutant plants were the same as wild type, the growth rate of the Kinesin-5 B mutant was slightly faster than the wild type, suggesting that interphase microtubule organization in elongating root cells is possibly affected in this line. In the Kinesin-5 B mutant, the growth rate is very similar to the wild type for the first six days, but it then continues to accelerate while in the wild type and in the Kinesin-5 A mutant, the growth rate levels off after about eight days, as has been reported in other studies (Baluška *et al*., 2003). This indicates that either the meristem or the elongation zone is longer in the Kinesin-5 B mutant. If more cells were

dividing or elongating, then growth would be expected to accelerate for a longer time period. Interestingly, this slightly increased growth rate correlates with a higher degree of organization in the root cortical microtubules (Figure 15).

Cortical microtubules in the T-DNA mutant lines were organized in parallel arrays perpendicular to the long axis of the root, and appeared to be generally similar to the wild type cortical microtubules. In order to assess the organization and general orientation of cortical microtubules in elongating root cells, we measured the angle of microtubules relative to the long axis of the cell. The average orientation of the microtubules was similar amongst the wild type, the Kinesin-5 A mutant, and the Kinesin-5 B mutant. On the other hand, quantitative analysis of the range of net angles of microtubule orientation showed that the microtubules were on average more parallel in the Kinesin-5 B mutant line, but not significantly. Kinesin-5 B might increase the dynamics of microtubules leading to less organized cortical microtubules (Figure 20).

The effect of microtubules on cell expansion relies on microtubule dynamics as well as orientation, as demonstrated in studies in which stabilized microtubules caused root swelling (Baskin *et al*., 1994). Therefore, the small increase in growth rate in the Kinesin-5 B mutant could represent the effect of a combination of increased microtubule organization and altered microtubule dynamics. It might also be that the minor change in cortical microtubules organization at the cellular level, in a large number of cells, could cumulatively translate into a measureable difference in growth rate.

Specialized Cell Shapes

As well as elongating root cells, microtubules play a prominent role in controlling the shape of more elaborately shaped cells, like trichomes and pavement cells. Trichomes are specialized cells that require precise control over cytoskeleton-directed cell expansion. Because of this they are particularly sensitive to changes in the organization or dynamics of the cytoskeleton. Although previous studies have shown that disruptions to the cytoskeleton can have profound effects on trichome shape (Mathur and Chua, 2000; Mathur, 2004), it does not appear to be influenced by Kinesin-5 A or Kinesin-5 B motor proteins.

It is evident that Kinesin-5 A is probably involved in pavement cell shape determination (i.e. the formation of interlocking lobes and troughs). Since the formation of pavement cells is a complex process involving multiple pathways, Kinesin-5 A could play a role in microtubule organization by cross liking, actin-microtubule interaction, or cell-to-cell signaling (Fu *et al*., 2002). It might be that, since there is less cross linking in the Kinesin-5 A mutant, the microtubules form fewer or looser bundles in the neck of the pavement cells resulting in less defined lobes (Figure 20).

Further evidence that Kinesin-5A might play a role in bundling of microtubules in pavement cells is that it is co-expressed with a GTPase that is part of the pathway that is known to control lobe formation. According to ATTED II Version 5.5 (Obayashi and Kinoshita, 2010) there is a correlation of 0.8 between Kinesin-5A and ROPGEF6; Rho guanyl-nucleotide exchange factor of ROPGTPase (Thomas *et al*., 2001). This Rho might be part of the ROP GTPase signaling pathway known to play a key role in the control of pavement cell shape (Fu *et al*., 2005). ROP interacts with RIC1 and RIC4. Regions of the

pavement cell that have activated ROP-RIC4 signal have actin networks which form the lobe and regions with ROP-RIC1 activation have organized microtubules which restricts lobing. This spatial isolation of signals results in extending and non-extending parts of the cell cortex allowing for lobe formation. The Kinesin-5 A mutant probably contributes to the bundling of microtubules in the non-extending area of the pavement cell, although our results don't show direct evidence of affected bundles in pavement cells (Figure 17).

Imaging microtubules in leaves is problematic because of the cuticle, which makes penetration of fixing agents and antibodies difficult. Many cells were not stained at all, and those that were stained were often cracked or broken, which allowed the antibodies in. These problems can potentially cause damage to sub-cellular structures during fixation. However, the images obtained are similar to those published previously (Barton *et al*., 2010) and to images of GFP-tubulin in living Arabidopsis leaves (Fu *et al*., 2005), suggesting that the protocol provided an accurate picture of the microtubules in stained cells. The microtubules in fixed and immunolabeled leaves looked the same in the mutants as in the wild type. However, because microtubules are less regularly organized in pavement cells than in root cells, it is difficult to identify subtle changes in microtubule organization, even though they may be sufficient to influence cell shape.

Conclusion

Although more investigation is warranted to further elucidate the role of Kinesin-5 members, it might be that these kinesins are not redundant for some functions, such as the pavement cell lobing, root cell cortical microtubule organization and the different mitotic stages. When looking at tissue level expression on EFP browser (Winter *et al.*,

2007) Kinesin-5 A and Kinesin-5 B are not expressed in the same area of the plant. They have different expression levels in the stomata, root elongation zone, cork and xylem (Figure 21). Judging from this and the results of this study, it could be concluded that they individually have different minor roles in different tissues.

While performing different minor roles in the different tissues might be true it doesn't rule out the possibility that these motors are partially redundant, considering that many plants don't carry both of them. They might be redundant for some functions in other areas judging from their expression patterns (Figure 21). Arabidopsis eFP browser relative output for Kinesin-5 A and Kinesin-5 B shows that expression levels are about the same during the different developmental stages, indicating that these two motor proteins might be redundant or that they work together to perform some functions.

A.

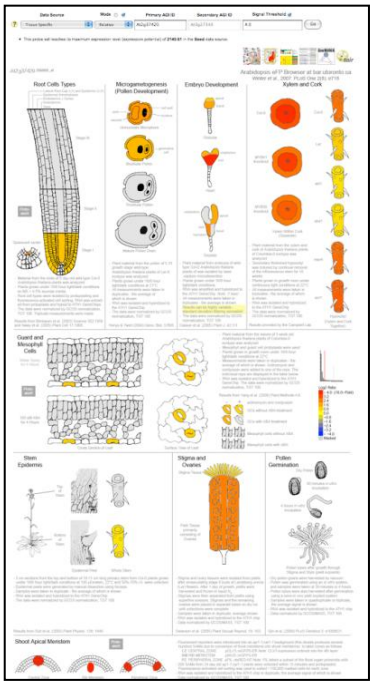

B.

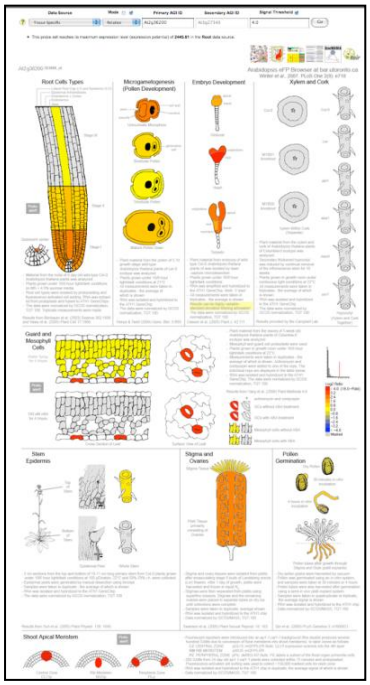

C.

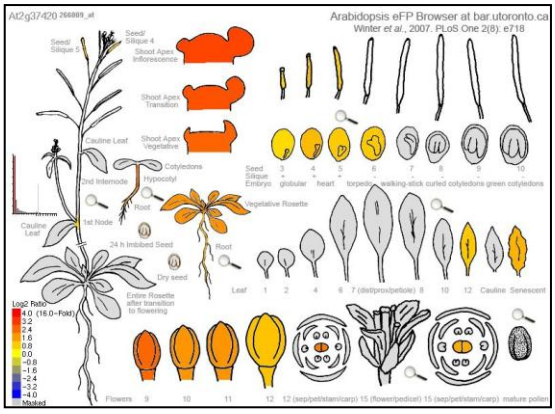

D.

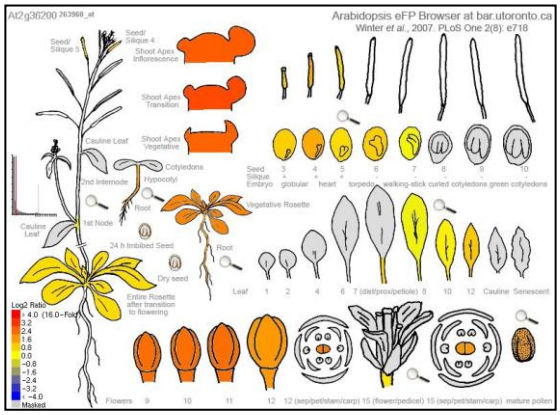

Figure 21. Relative expression levels of Kinesin-5 A and Kinesin-5 B from the Arabidopsis eFP browser. A. Tissue level expression pattern for Kinesin-5 A gene. B. Tissue level expression pattern for Kinesin-5 B gene. C-D. Developmental pattern of gene expression for Kinesin-5 A and Kinesin-5 B respectively. Threshold is set to 4 giving a color scale of -4 to 4 expression level compared to median levels with Blue to Red indicating the scale on the sample. The Gray indicates values less than 20 which is the detection background level.

Arabidopsis Kinesin-5 members A and B appear to perform different functions during different cell stages. During mitosis Kinesin-5 A influences metaphase and cytokinesis while Kinesin-5 B affects the pre-prophase band and anaphase progression. How they influence the phenotypes of cells is still a mystery. We speculate that Arabidopsis Kinesin-5 A is involved in cross linking microtubules and Kinesin-5 B affects the dynamics of microtubules during interphase. It is not surprising to find that these kinesins have multiple roles, be they minor. Another member of this family, Kinesin-5 C, is known for its role in metaphase and interphase microtubule organization. What is missing is the role of Kinesin-5 D. The lack of a D mutant reveals a need for further research into this gene to find out what is the significant role it most likely plays in the plant cell. Screening more insertion lines or performing site-directed mutagenesis might result in finding a Kinesin-5 D mutant.

The Arabidopsis Kinesin-5 family members are now a little less enigmatic. To further this study, phenotypic analysis of other plant structures influenced by microtubule organization such as the elongating hypocotyl, root hairs, and reproductive structures would expose if these Kinesin-5 members function anywhere else besides pavement cell, elongating root cell and some mitotic stages.

V. References

Alonso, J. M., Stepanova, A. N., Leisse, T. J., Kim, C. J., Chen, H., Shinn, P., Stevenson, D. K., Zimmerman, J., Barajas, P., Cheuk, R. *et al*. (2003). Genome-wide insertional mutagenesis of arabidopsis thaliana. *Science* **301,** 653-657.

Ambrose, J. C. and Cyr, R. (2007). The kinesin ATK5 functions in early spindle assembly in arabidopsis. *Plant Cell* **19,** 226-236.

Ambrose, J. C., Li, W., Marcus, A., Ma, H. and Cyr, R. (2005). A minus-end-directed kinesin with plus-end tracking protein activity is involved in spindle morphogenesis. *Mol. Biol. Cell* **16,** 1584-1592.

Asada, T., Kuriyama, R. and Shibaoka, H. (1997). TKRP125, a kinesin-related protein involved in the centrosome-independent organization of the cytokinetic apparatus in tobacco BY-2 cells. *J. Cell. Sci.* **110,** 179-189.

Asada, T., Sonobe, S. and Shibaoka, H. (1991). Microtubule translocation in the cytokinetic apparatus of cultured tobacco cells. *Nature* **350,** 238-241.

Baluška, F., Wojtaszek, P., Volkmann, D. and Barlow, P. (2003). The architecture of polarized cell growth: The unique status of elongating plant cells. *Bioessays* **25,** 569-576.

Bannigan, A., Lizotte-Waniewski, M., Riley, M. and Baskin, T. I. (2008). Emerging molecular mechanisms that power and regulate the anastral mitotic spindle of flowering plants. *Cell Motil. Cytoskeleton* **65,** 1-11.

Bannigan, A., Scheible, W. -., Lukowitz, W., Fagerstrom, C., Wadsworth, P., Somerville, C. and Baskin, T. I. (2007). A conserved role for kinesin-5 in plant mitosis. *J. Cell. Sci.* **120,** 2819-2827.

Barroso, C., Chan, J., Allan, V., Doonan, J., Hussey, P. and Lloyd, C. (2000). Two kinesin-related proteins associated with the cold-stable cytoskeleton of carrot cells: Characterization of a novel kinesin, DcKRP120-2. *Plant Journal* **24,** 859-868.

Barton, D. A. and Overall, R. L. (2010). Cryofixation rapidly preserves cytoskeletal arrays of leaf epidermal cells revealing microtubule co-alignments between neighbouring cells and adjacent actin and microtubule bundles in the cortex. *J. Microsc.* **237,** 79-88.

Baskin, T. I. (2001). On the alignment of cellulose microfibrils by cortical microtubules: A review and a model. *Protoplasma* **215,** 150-171.

Baskin, T. I. (2005). Anisotropic expansion of the plant cell wall. *Annual Review of Cell and Developmental Biology* **21,** 203-222.

Baskin, T. I., Meekes, H. T. H. M., Liang, B. M. and Sharp, R. E. (1999). Regulation of growth anisotropy in well-watered and water-stressed maize roots. II. role of cortical microtubules and cellulose microfibrils. *Plant Physiol.* **119,** 681-692.

Baskin, T. I., Wilson, J. E., Cork, A. and Williamson, R. E. (1994). Morphology and microtubule organization in arabidopsis roots exposed to oryzalin or taxol. *Plant and Cell Physiology* **35,** 935-942.

Beemster, G. T. S. and Baskin, T. I. (1998). Analysis of cell division and elongation underlying the developmental acceleration of root growth in arabidopsis thaliana. *Plant Physiol.* **116,** 1515-1526.

Bibikova, T. N., Blancaflor, E. B. and Gilroy, S. (1999). Microtubules regulate tip growth and orientation in root hairs of arabidopsis thaliana. *Plant Journal* **17,** 657-665.

Bichet, A., Desnos, T., Turner, S., Grandjean, O. and Ho¨fte, H. (2001). BOTERO1 is required for normal orientation of cortical microtubules and anisotropic cell expansion in arabidopsis. *Plant Journal* **25,** 137-148.

Brady, S. T. (1985). A novel brain ATPase with properties expected for the fast axonal transport motor. *Nature* **317,** 73-75.

Burk, D. H., Liu, B., Zhong, R., Morrison, W. H. and Ye, Z. -. (2001). A katanin-like protein regulates normal cell wall biosynthesis and cell elongation. *Plant Cell* **13,** 807-827.

Buschmann, H. and Lloyd, C. W. (2008). Arabidopsis mutants and the network of microtubule-associated functions. *Molecular Plant* **1,** 888-898.

Cai, G., Bartalesi, A., Del Casino, C., Moscatelli, A., Tiezzi, A. and Cresti, M. (1993). The kinesin-immunoreactive homologue from nicotiana tabacum pollen tubes: Biochemical properties and subcellular localization. *Planta* **191,** 496-506.

Cole, D. G., Saxton, W. M., Sheehan, K. B. and Scholey, J. M. (1994). A 'slow' homotetrameric kinesin-related motor protein purified from drosophila embryos. *J. Biol. Chem.* **269,** 22913-22916.

Dagenbach, E. M. and Endow, S. A. (2004). A new kinesin tree. *J. Cell. Sci.* **117,** 3-7.

Desai, A. and Mitchison, T. J. (1997). Microtubule polymerization dynamics. *Annual Review of Cell and Developmental Biology* **13,** 83-117.

Ehrhardt, D. W. and Shaw, S. L. (2006). Microtubule dynamics and organization in the plant cortical array. *Annual Review of Plant Biology* **57,** 859-875.

Ferenz, N. P., Gable, A. and Wadsworth, P. (2010). Mitotic functions of kinesin-5. *Seminars in Cell and Developmental Biology* **21,** 255-259.

Folkers, U., Berger, J. and Hülskamp, M. (1997). Cell morphogenesis of trichomes in arabidopsis: Differential control of primary and secondary branching by branch initiation regulators and cell growth. *Development* **124,** 3779-3786.

Fu, Y., Gu, Y., Zheng, Z., Wasteneys, G. and Yang, Z. (2005). Arabidopsis interdigitating cell growth requires two antagonistic pathways with opposing action on cell morphogenesis. *Cell* **120,** 687-700.

Fu, Y., Li, H. and Yang, Z. (2002). The ROP2 GTPase controls the formation of cortical fine F-actin and the early phase of directional cell expansion during arabidopsis organogenesis. *Plant Cell* **14,** 777-794.

Gatlin, J. C. and Bloom, K. (2010). Microtubule motors in eukaryotic spindle assembly and maintenance. *Seminars in Cell and Developmental Biology* **21,** 248-254.

Gelfand, V. I. and Bershadsky, A. D. (1991). Microtubule dynamics: Mechanism, regulation, and function. *Annu. Rev. Cell Biol.* **7,** 93-116.

Guo, L., Ho, C. -. K., Kong, Z., Lee, Y. -. J., Qian, Q. and Liu, B. (2009). Evaluating the microtubule cytoskeleton and its interacting proteins in monocots by mining the rice genome. *Annals of Botany* **103,** 387-402.

Hashimoto, T. (2003). Dynamics and regulation of plant interphase microtubules: A comparative view. *Curr. Opin. Plant Biol.* **6,** 568-576.

Hayashi, T., Sano, T., Kutsuna, N., Kumagai-Sano, F. and Hasezawa, S. (2007). Contribution of anaphase B to chromosome separation in higher plant cells estimated by image processing. *Plant and Cell Physiology* **48,** 1509-1513.

Hentrich, C. and Surrey, T. (2010). Microtubule organization by the antagonistic mitotic motors kinesin-5 and kinesin-14. *J. Cell Biol.* **189,** 465-480.

Hepler, P. K. and Hush, J. M. (1996). Behavior of microtubules in living plant cells. *Plant Physiol.* **112,** 455-461.

Hepler, P. K., Valster, A., Molchan, T. and Vos, J. W. (2002). Roles for kinesin and myosin during cytokinesis. *Philosophical Transactions of the Royal Society B: Biological Sciences* **357,** 761-766.

Hülskamp, M., Miséra, S. and Jürgens, G. (1994). Genetic dissection of trichome cell development in arabidopsis. *Cell* **76,** 555-566.

Jaffe, A. B. and Hall, A. (2005). Rho GTPases: Biochemistry and biology. *Annual Review of Cell and Developmental Biology* **21,** 247-269.

Kapitein, L. C., Peterman, E. J. G., Kwok, B. H., Kim, J. H., Kapoor, T. M. and Schmidt, C. F. (2005). The bipolar mitotic kinesin Eg5 moves on both microtubules that it crosslinks. *Nature* **435,** 114-118.

Kaul, S., Koo, H. L., Jenkins, J., Rizzo, M., Rooney, T., Tallon, L. J., Feldblyum, T., Nierman, W., Benito, M. -., Lin, X. *et al*. (2000). Analysis of the genome sequence of the flowering plant arabidopsis thaliana. *Nature* **408,** 796-815.

Kellogg, D. R., Moritz, M. and Alberts, B. M. (1994). The centrosome and cellular organization. *Annu. Rev. Biochem.* **63,** 639-674.

Kost, B., Mathur, J. and Chua, N. -. (1999). Cytoskeleton in plant development. *Curr. Opin. Plant Biol.* **2,** 462-470.

Kotzer, A. M. and Wasteneys, G. O. (2006). Mechanisms behind the puzzle: Microtubule-microfilament cross-talk in pavement cell formation. *Canadian Journal of Botany* **84,** 594-603.

Lagomarsino, M. C., Tanase, C., Vos, J. W., Emons, A. M. C., Mulder, B. M. and Dogterom, M. (2007). Microtubule organization in three-dimensional confined geometries: Evaluating the role of elasticity through a combined in vitro and modeling approach. *Biophys. J.* **92,** 1046-1057.

Larkin, J. C., Young, N., Prigge, M. and Marks, M. D. (1996). The control of trichome spacing and number in arabidopsis. *Development* **122,** 997-1005.

Lawrence, C. J., Dawe, R. K., Christie, K. R., Cleveland, D. W., Dawson, S. C., Endow, S. A., Goldstein, L. S. B., Goodson, H. V., Hirokawa, N., Howard, J. *et al*. (2004). A standardized kinesin nomenclature. *J. Cell Biol.* **167,** 19-22.

Lawrence, C. J., Morris, N. R., Meagher, R. B. and Dawe, R. K. (2001). Dyneins have run their course in plant lineage. *Traffic* **2,** 362-363.

Lebedeva, L. I., Fedorova, S. A., Trunova, S. A. and Omelyanchuk, L. V. (2004). Mitosis: Regulation and organization of cell division. *Russian Journal of Genetics* **40,** 1313-1330.

Lloyd, C. and Chan, J. (2006). Not so divided: The common basis of plant and animal cell division. *Nature Reviews Molecular Cell Biology* **7,** 147-152.

Loughner, R., Wentworth, K., Loeb, G. and Nyrop, J. (2010). Leaf trichomes influence predatory mite densities through dispersal behavior. *Entomol. Exp. Appl.* **134,** 78-88.

Marcus, A. I., Li, W., Ma, H. and Cyr, R. J. (2003). A kinesin mutant with an atypical bipolar spindle undergoes normal mitosis. *Mol. Biol. Cell* **14,** 1717-1726.

Mathur, J. (2004). Cell shape development in plants. *Trends Plant Sci.* **9,** 583-590.

Mathur, J. and Chua, N. -. (2000). Microtubule stabilization leads to growth reorientation in arabidopsis trichomes. *Plant Cell* **12,** 465-477.

Miki, H., Okada, Y. and Hirokawa, N. (2005). Analysis of the kinesin superfamily: Insights into structure and function. *Trends Cell Biol.* **15,** 467-476.

Mineyuki, Y. (1999). The preprophase band of microtubules: Its function as a cytokinetic apparatus in higher plants. *International Review of Cytology* **187,** 1-49.

Müller, S., Wright, A. J. and Smith, L. G. (2009). Division plane control in plants: New players in the band. *Trends Cell Biol.* **19,** 180-188.

Obayashi, T. and Kinoshita, K. (2010). Coexpression landscape in ATTED-II: Usage of gene list and gene network for various types of pathways. *J. Plant Res.* **123,** 311-319.

Page, R. D. M. (1996). TreeView: An application to display phylogenetic trees on personal computers. *Computer Applications in the Biosciences* **12,** 357-358.

Qian, P., Hou, S. and Guo, G. (2009). Molecular mechanisms controlling pavement cell shape in arabidopsis leaves. *Plant Cell Rep.* **28,** 1147-1157.

Reddy, A. S. N. and Day, I. S. (2001). Kinesins in the arabidopsis genome: A comparative analysis among eukaryotes. *BMC Genomics* **2,**.

Richardson, D. N., Simmons, M. P. and Reddy, A. S. N. (2006). Comprehensive comparative analysis of kinesins in photosynthetic eukaryotes. *BMC Genomics* **7,**.

Saitou, N. and Nei, M. (1987). The neighbor-joining method: A new method for reconstructing phylogenetic trees. *Mol. Biol. Evol.* **4,** 406-425.

Saunders, A. M., Powers, J., Strome, S. and Saxton, W. M. (2007). Kinesin-5 acts as a brake in anaphase spindle elongation. *Current Biology* **17,** R453-R454.

Schmit, A. -C. (2002). Acentrosomal microtubule nucleation in higher plants. *International Review of Cytology* **220,** 257-289.

Schwab, B., Folkers, U., Ilgenfritz, H. and Hülskamp, M. (2000). Trichome morphogenesis in arabidopsis. *Philosophical Transactions of the Royal Society B: Biological Sciences* **355,** 879-883.

Seltzer, V., Pawlowski, T., Campagne, S., Canaday, J., Erhardt, M., Evrard, J. -., Herzog, E. and Schmit, A. -. (2003). Multiple microtubule nucleation sites in higher plants. *Cell Biol. Int.* **27,** 267-269.

Sharp, D. J., Rogers, G. C. and Scholey, J. M. (2000). Microtubule motors in mitosis. *Nature* **407,** 41-47.

Smith, L. G. and Oppenheimer, D. G. (2005). Spatial control of cell expansion by the plant cytoskeleton. *Annual Review of Cell and Developmental Biology* **21,** 271-295.

Thomas, C., Fricke, I., Scrima, A., Berken, A. and Wittinghofer, A. (2007). Structural evidence for a common intermediate in small G protein-GEF reactions. *Mol. Cell* **25,** 141-149.

Vale, R. D., Schnapp, B. J., Reese, T. S. and Sheetz, M. P. (1985). Movement of organelles along filaments dissociated from the axoplasm of the squid giant axon. *Cell* **40,** 449-454.

Vassileva, V. N., Fujii, Y. and Ridge, R. W. (2005). Microtubule dynamics in plants. *Plant Biotechnology* **22,** 171-178.

Wasteneys, G. O. and Ambrose, J. C. (2009). Spatial organization of plant cortical microtubules: Close encounters of the 2D kind. *Trends Cell Biol.* **19,** 62-71.

Wasteneys, G. O., Willingale-Theune, J. and Menzel, D. (1997). Freeze shattering: A simple and effective method for permeabilizing higher plant cell walls. *J. Microsc.* **188,** 51-61.

Wasteneys, G. O. and Yang, Z. (2004). New views on the plant cytoskeleton. *Plant Physiol.* **136,** 3884-3891.

Whittington, A. T., Vugrek, O., Wei, K. J., Hasenbein, N. G., Sugimoto, K., Rashbrooke, M. C. and Wasteneys, G. O. (2001). MOR1 is essential for organizing cortical microtubules in plants. *Nature* **411,** 610-613.

Wiedemeier, A. M. D., Judy-March, J. E., Hocart, C. H., Wasteneys, G. O., Williamson, R. E. and Baskin, T. I. (2002). Mutant alleles of arabidopsis RADIALLY SWOLLEN 4 and 7 reduce growth anisotropy without altering the transverse orientation of cortical microtubules or cellulose microfibrils. *Development* **129,** 4821-4830.

Winter, D., Vinegar, B., Nahal, H., Ammar, R., Wilson, G. V. and Provart, N. J. (2007). An "electronic fluorescent pictograph" browser for exploring and analyzing large-scale biological data sets. *PloS one* **2,**.

Zhang, D., Wadsworth, P. and Hepler, P. K. (1990). Microtubule dynamics in living dividing plant cells: Confocal imaging of microinjected fluorescent brain tubulin. *Proc. Natl. Acad. Sci. U. S. A.* **87,** 8820-8824.